resistance is associated with the plaque-type pathology of AD,[3] even though there are some controversial findings.[4,5]

Along with insulin resistance and diabetes, dyslipidemia is an important metabolic disorder. In humans, however, there are few studies regarding the association between dyslipidemia and AD-related pathology.[6,7] In this study, to clarify the relationship between abnormal lipid metabolism and AD, we searched for evidence of AD-related pathologic risk by examining the associations between lipid profiles and the typical AD-related pathologic outcomes, neuritic plaques (NPs) and neurofibrillary tangles (NFTs).

## METHODS

**Subjects.** The design of the Hisayama Study has been described in detail elsewhere.[3,8–10] In the present study, we examined a series of autopsy samples of Hisayama residents from October 1, 1998, to March 31, 2003. During this period, 290 residents in Hisayama died and 214 were autopsied (autopsy rate 73.8%). The clinical data for the present study were collected from a clinical examination performed in 1988, as described previously.[9] Briefly, of a total of 3,227 residents aged 40–79 years included in the study registry, 2,587 (participation rate, 80.2%) took part in a clinical examination in 1988. Of the 214 autopsy cases, we excluded 3 subjects whose brain specimens were inadequate for evaluation, and 64 subjects who did not complete the fasting blood protocol in 1988. Finally, 147 subjects who underwent both the fasting blood protocol and brain autopsy were included in the present study. None of the 147 subjects showed signs of dementia at the clinical examination in 1988. The study subjects mostly overlapped with those in our previous study, in which we reported the association of insulin resistance with the plaque-type pathology of AD.[3]

**Standard protocol approvals, registrations, and patient consents.** The study was approved by the Ethics Committee of the Faculty of Medicine, Kyushu University, and was performed in accordance with the ethical standards described in the 5th revision of the Declaration of Helsinki, 2000. Written informed consent was obtained from all study subjects.

**Risk factors.** In the clinical examination performed in 1988, blood samples were collected on the morning after an overnight fast. We used values of total cholesterol (TC), low-density lipoprotein cholesterol (LDLC), high-density lipoprotein cholesterol (HDLC), triglycerides (TG), TC/HDLC, LDLC/HDLC, and non-HDLC as lipid profiles. Levels of TC, HDLC, and TG were determined enzymatically. LDLC was calculated using the Friedewald formula (LDLC = TC − HDLC − TG/5).[11] Non-HDLC was defined as non-HDLC = TC − HDLC. Other risk factors were also measured as described previously.[3] *APOE* genotyping was determined by direct sequencing. The homozygous ϵ4 genotype was not found among these participants, and those who carried one copy of the ϵ4 allele were categorized as *APOE* ϵ4 carriers.

**Assessment of neuropathologic changes.** Brain specimens in each case included the middle frontal gyrus, superior and middle temporal gyri, inferior parietal lobule, anterior cingulated gyrus, amygdala, hippocampus with entorhinal and transentorhinal cortex, calcarine cortex, basal ganglia including the nucleus basalis of Meynert, thalamus, substantia nigra, locus ceruleus, and dorsal vagal nucleus. Sections were routinely stained using hematoxylin-eosin, Klüver-Barrera stain, and a modified Bielschowsky method. Specimens from each subject were immunostained with antibodies against phosphorylated tau (AT8, mouse monoclonal, 1:500; Innogenetics, Belgium). The assessment of AD pathology was conducted according to the Consortium to Establish a Registry for Alzheimer's Disease (CERAD) guidelines[12] and to Braak stage.[13,14] For the pathologic assessment of cerebrovascular diseases, any type of cerebral infarction or hemorrhage was recorded according to gross examination and microscopic assessment, regardless of clinical features.

**Statistical analyses.** Mean or geometric mean values of continuous data among the NP or NFT groups were adjusted for age and sex and compared by analysis of covariance. Proportions of categorical data were adjusted for age and sex by direct method and compared by logistic regression analysis. We also used logistic regression analysis to determine relationships between risk factors and pathologic outcome, which are expressed as odds ratios (OR) and 95% confidence intervals (CI). Model 1 was adjusted for age and sex. Model 2 was adjusted for model 1 plus systolic blood pressure, fasting blood glucose levels, fasting insulin levels, body mass index, smoking habit, regular exercise, and cerebrovascular disease. Model 3 was adjusted for model 2 plus *APOE* ϵ4 carrier.

Each lipid profile was divided into 4 groups to compare the risk of NPs among quartiles. Missing values (2 for LDL cholesterol, 1 for fasting insulin levels, 7 for *APOE* ϵ4 carrier, and 1 for the grading of Braak stage) were excluded from the analysis. In addition, subjects were divided into high or low groups at the boundary of the most unfavorable quartile to compare the risk of NPs. Significance was defined as $p < 0.05$.

## RESULTS

The demographic characteristics of the study subjects at clinical examination are described in table 1. The mean age at death was 76 years in subjects without NPs (CERAD = 0) and 83 years in those with NPs (CERAD = 1 to 3). There was no clear selection bias regardless of autopsy, according to a comparison of demographic characteristics between our study subjects and those who did not undergo autopsy (data not shown). After the clinical examination in 1988, 34.0% (n = 50) of subjects developed dementia; specifically, 17.7% (n = 26) were Alzheimer-type dementia, 13.6% (n = 20) were vascular dementia, and 2.0% (n = 3) were mixed-type dementia.

The frequencies of NPs were categorized into the following 4 groups by CERAD criteria: 32.0% (n = 47) for none (score 0), 15.7% (n = 23) for sparse (score 1), 15.0% (n = 22) for moderate (score 2), and 37.4% (n = 55) for frequent (score 3). The extent of NFTs was classified into the following 4 groups by Braak stage: 13.0% (n = 19) for stage 0, 17.8% (n = 26) for stage I to II, 43.8% (n = 64) for stage III to IV, and 25.3% (n = 37) for stage V to VI. Prevalence of cerebrovascular disease at autopsy

Table 1 **Demographic characteristics of 147 subjects according to the presence of NPs or NFTs[a]**

| Variables | Without NPs (CERAD = 0) (n = 47) | With NPs (CERAD = 1 to 3) (n = 100) | Without NFTs (Braak stage = 0) (n = 19) | With NFTs (Braak stage = I to VI) (n = 127) |
|---|---|---|---|---|
| Male sex, % | 41.9 | 46.5 | 51.3 | 43.9 |
| Age at medical examination, y | 63 ± 1 | 71 ± 1[b] | 62 ± 2 | 69 ± 1[b] |
| Fasting plasma glucose, mmol/L | 5.7 ± 0.2 | 6.0 ± 0.1 | 5.6 ± 0.3 | 5.9 ± 0.1 |
| Fasting insulin, μU/mL | 4.5 (4.0, 5.2) | 5.5 (5.0, 6.0)[b] | 5.1 (4.1, 6.2) | 5.2 (4.8, 5.6) |
| Systolic blood pressure, mm Hg | 143.3 ± 3.6 | 137.5 ± 2.4 | 135.4 ± 5.7 | 139.8 ± 2.1 |
| Diastolic blood pressure, mm Hg | 78.1 ± 1.9 | 76.0 ± 1.3 | 76.4 ± 2.9 | 76.5 ± 1.1 |
| TC, mmol/L | 4.9 ± 0.2 | 5.4 ± 0.1[b] | 5.5 ± 0.3 | 5.2 ± 0.1 |
| LDLC, mmol/L | 3.0 ± 0.2 | 3.6 ± 0.1[b] | 3.8 ± 0.2 | 3.4 ± 0.1 |
| HDLC, mmol/L | 1.4 ± 0.1 | 1.3 ± 0.03 | 1.3 ± 0.1 | 1.3 ± 0.0 |
| TG, mmol/L | 1.0 (0.9, 1.2) | 1.2 (1.1, 1.3) | 1.1 (0.9, 1.4) | 1.1 (1.0, 1.2) |
| TC/HDLC | 3.7 ± 0.2 | 4.6 ± 0.1[b] | 4.5 ± 0.3 | 4.3 ± 0.1 |
| LDLC/HDLC | 2.4 ± 0.2 | 3.0 ± 0.1[b] | 3.0 ± 0.3 | 2.8 ± 0.1 |
| Non-HDLC, mmol/L | 3.5 ± 0.2 | 4.2 ± 0.1[b] | 4.2 ± 0.3 | 3.9 ± 0.1 |
| Body mass index, kg/m$^2$ | 21.8 ± 0.5 | 21.9 ± 0.3 | 21.6 ± 0.7 | 21.9 ± 0.3 |
| Current smoking, % | 49.5 | 43.6 | 59.4 | 40.3 |
| Regular exercise, % | 6.6 | 5.2 | 0.2 | 8.6 |
| *APOE* ε4 carrier, % | 0.03 | 21.8[b] | 17.6 | 14.5 |

Abbreviations: CERAD = Consortium to Establish a Registry for Alzheimer's Disease; HDLC = high-density lipoprotein cholesterol; LDLC = low-density lipoprotein cholesterol; NFT = neurofibrillary tangle; NP = neuritic plaque; TC = total cholesterol; TG = triglycerides.

[a] Values are %, mean ± SE, or geometric mean (95% prediction interval). Geometric means of fasting insulin and triglycerides are shown due to the skewed distribution. Values are adjusted for age and sex except for sex and age at medical examination.

[b] $p < 0.05$. Male sex is adjusted for age. Age at medical examination is adjusted for sex.

was 59.2% (n = 87), which included any type of infarction (n = 73), hemorrhage (n = 10), or Binswanger type change (n = 6).

As shown in tables 2 and 3, we compared adjusted mean or geometric mean values of each lipid profile among groups according to CERAD score for NPs or Braak stage for NFTs. In the age- and sex-adjusted analyses (model 1), the subjects with NPs (CERAD score 1 to 3) showed significantly higher TC, LDLC, TC/HDLC, LDLC/HDLC, and non-HDLC levels compared to subjects without NPs (CERAD score 0). These associations remained significant even after multivariate model analysis (model 2 and 3). Test for trend among 4 CERAD stages revealed a limited dose-response relationship after multivariate model analysis. Unfavorable lipid metabolism was significantly associated with plaque-type AD pathology even in sparse to moderate stages (CERAD = 1 or 2). In contrast, we found no significant association between any lipid profile and NFT pathology (Braak stage I to VI vs stage 0).

To confirm these associations, we compared the risk of NPs among quartiles of each lipid profile in table 4. Compared with the lowest quartile (Q1) of TC, age- and sex-adjusted risks of NPs (model 1) were constant in the second (Q2) and the third (Q3) quartiles, but were significantly increased in the highest quartile (Q4). This relationship remained significant even after multivariate adjustment (model 2). Further adjustment for *APOE* genotype resulted in a higher increased risk of NPs (model 3). In a similar way, the highest quartiles of LDLC, TC/HDLC, LDLC/HDLC, and non-HDLC showed increased risk for NPs compared with the lowest respective quartiles. These findings suggested that the relationship between lipid profiles and the presence of NPs may fit with threshold models but not with linear models.

Additionally, table 4 shows ORs for the presence of NPs relative to lipid profile levels, namely low or high. We set the threshold level between Q3 and Q4 (lipid profiles excluding HDLC) or between Q1 and Q2 (HDLC). NPs were found in 86.1% of subjects with high TC (>5.80 mmol/L) and in 62.2% of people with low TC (≤5.80 mmol/L). Compared with low TC, the age- and sex-adjusted risk of NPs was significantly increased for high TC (model 1). After multivariate adjustments (models 2 and 3), this relationship remained significant. In a similar way, high levels of LDLC, TC/HDLC, LDLC/HDLC, and non-HDLC showed significantly increased risk for NPs compared with low levels, even after multivariate adjustments. When we performed similar analyses in which we narrow down the subjects with NPs to the group of CERAD = 2 to 3 (table e-1 on the *Neurology*® Web site at www.neurology.org) or CERAD = 3 (table e-2), similar associations between the lipid profiles and NPs were observed. The similar findings were observed even in the sensitivity analyses that excluded 26 cases with Alzheimer-type dementia (table e-3), or those that excluded 28 *APOE* ε4 carriers (data not shown). Because of the limited sample size, we could not perform sex-specific analyses.

**DISCUSSION** Using a series of autopsy cases from a general Japanese population, we found that high levels of TC, LDLC, TC/HDLC, LDLC/HDLC, and non-HDLC were significantly associated with plaque-type AD pathology. Our findings also suggest that the relationship between these lipid profiles and NPs may have certain threshold levels.

Because lipid metabolism is closely related to *APOE* genotype,[15] which is a strong risk factor for AD pathogenesis,[16] we compared the results of 2 multivariate models (model 2 and 3). The relationship between HDLC levels and the risk of NPs was diminished after adjustment for *APOE* genotype,

Table 2 Adjusted mean or geometric mean values of each lipid profile according to CERAD score[a]

| | Model 1 | | | | | | Model 2 | | | | | | Model 3 | | | | | |
|---|---|---|---|---|---|---|---|---|---|---|---|---|---|---|---|---|---|---|
| | CERAD score | | | | | | CERAD score | | | | | | CERAD score | | | | | |
| | 0 (n = 47) | 1 (n = 23) | 2 (n = 22) | 3 (n = 55) | p for trend | p (1–3 vs 0) | 0 (n = 47) | 1 (n = 23) | 2 (n = 22) | 3 (n = 55) | p for trend | p (1–3 vs 0) | 0 (n = 47) | 1 (n = 23) | 2 (n = 22) | 3 (n = 55) | p for trend | p (1–3 vs 0) |
| TC, mmol/L | 4.87 | 5.47[b] | 5.66[b] | 5.32 | 0.07 | 0.006 | 4.85 | 5.47[b] | 5.70[b] | 5.34[b] | 0.05 | 0.005 | 4.82 | 5.42[b] | 5.69[b] | 5.36 | 0.049 | 0.005 |
| LDLC, mmol/L | 3.05 | 3.54 | 3.83[b] | 3.46 | 0.07 | 0.008 | 3.02 | 3.55 | 3.86[b] | 3.47[b] | 0.05 | 0.005 | 3.01 | 3.53 | 3.85[b] | 3.50 | 0.05 | 0.007 |
| HDLC, mmol/L | 1.36 | 1.25 | 1.33 | 1.23 | 0.08 | 0.09 | 1.35 | 1.29 | 1.33 | 1.22 | 0.11 | 0.20 | 1.31 | 1.26 | 1.33 | 1.26 | 0.62 | 0.63 |
| TG, mmol/L | 1.00 | 1.30 | 0.99 | 1.22 | 0.20 | 0.09 | 1.02 | 1.25 | 1.00 | 1.22 | 0.25 | 0.18 | 1.06 | 1.25 | 1.01 | 1.15 | 0.77 | 0.49 |
| TC/HDLC | 3.73 | 4.64[b] | 4.47[b] | 4.56[b] | 0.006 | 0.001 | 3.76 | 4.51[b] | 4.50[b] | 4.59[b] | 0.004 | 0.001 | 3.87 | 4.58[b] | 4.51 | 4.50[b] | 0.05 | 0.009 |
| LDLC/HDLC | 2.39 | 2.93[b] | 3.06[b] | 2.96[b] | 0.01 | 0.003 | 2.38 | 2.87 | 3.07[b] | 2.99[b] | 0.008 | 0.003 | 2.45 | 2.92 | 3.07[b] | 2.94 | 0.06 | 0.02 |
| Non-HDLC, mmol/L | 3.51 | 4.21[b] | 4.33[b] | 4.10[b] | 0.02 | 0.001 | 3.50 | 4.18[b] | 4.37[b] | 4.12[b] | 0.01 | 0.001 | 3.51 | 4.16[b] | 4.36[b] | 4.10[b] | 0.03 | 0.002 |

Abbreviations: CERAD = Consortium to Establish a Registry for Alzheimer's Disease; HDLC = high-density lipoprotein cholesterol; LDLC = low-density lipoprotein cholesterol; TC = total cholesterol; TG = triglycerides.

[a] Model 1 was adjusted for age and sex. Model 2 was adjusted for age, sex, systolic blood pressure, fasting blood glucose, fasting insulin, body mass index, current smoking, regular exercise, and cerebrovascular disease. Model 3 was adjusted for age, sex, systolic blood pressure, fasting blood glucose, fasting insulin, body mass index, current smoking, regular exercise, cerebrovascular disease, and *APOE* ε4 carrier. Geometric mean of triglyceride is shown due to the skewed distribution.

[b] $p < 0.05$ vs CERAD score = 0.

which suggested that *APOE* genotype was a confounding factor that had distorted the relationship between HDLC and NPs. Meanwhile, adjustment for *APOE* genotype resulted in a greater increased risk of NPs in association with high levels of TC, LDLC, and non-HDLC. These findings indicated that lipid profiles, such as TC, LDLC, and non-HDLC, may be significant risk factors for NPs and that these relationships were independent from *APOE* genotype.

There was a limited dose-response relationship between the lipid profiles and CERAD score after multivariate model analysis, which might be diminished by an epidemiologic competing effect, indicating that subjects with very high lipid profiles at the clinical examination probably died earlier as a result of cardiovascular disease, for example. Moreover, there might be a threshold effect, indicating that serum cholesterol in excess of a certain threshold level would trigger the plaque formation even though the further development of AD pathology might be modified by different factors. To control the serum cholesterol below a threshold level would decrease the risk of plaque formation, which might contribute to the prevention of AD.

Our analyses using quartiles suggested possible threshold levels to be approximately 6 mmol/L for TC and 4 mmol/L for LDLC. TC/HDLC, LDLC/HDLC, and non-HDLC are primarily the indexes for prediction of coronary heart disease based on a linear relationship[17]; nevertheless, our results also showed certain threshold levels for these indexes. This suggests that the increased risk of NP formation is less associated with atherosclerotic vascular factors. Lipid profiles were measured in blood samples; however, peripheral lipid profiles could be quite different from cholesterol metabolism in the brain. There may be a homeostatic regulation of cholesterol across the blood–brain barrier, which might adopt a threshold in the periphery. It is difficult to further estimate exact threshold levels due to the limited sample size of this study. Further studies with a larger sample size are needed to determine this issue.

The absence of a consistent association between the lipid profiles and NFT pathology in the present study might be due to the relatively small sample size; nevertheless, NFT pathology was less associated with disturbed lipid metabolism than was the formation of NPs, and NFT pathology is considered to be a consequence of A$\beta$ deposition in the amyloid cascade hypothesis.[18] Lipid profiles may act upstream of the cascade, and might trigger AD pathogenesis. This is similar to the relationship between diabetes-related factors and NP pathology that we have previously reported.[3] The dissociation with the NFT could be

Table 3 Adjusted mean or geometric mean values of each lipid profile according to Braak and Braak staging[a]

| | Model 1 | | | | | | Model 2 | | | | | | Model 3 | | | | | |
|---|---|---|---|---|---|---|---|---|---|---|---|---|---|---|---|---|---|---|
| | Braak stage | | | | | | Braak stage | | | | | | Braak stage | | | | | |
| | 0 (n = 19) | I, II (n = 26) | III, IV (n = 64) | V, VI (n = 37) | p for trend | p (I–VI vs 0) | 0 (n = 19) | I, II (n = 26) | III, IV (n = 64) | V, VI (n = 37) | p for trend | p (I–VI vs 0) | 0 (n = 19) | I, II (n = 26) | III, IV (n = 64) | V, VI (n = 37) | p for trend | p (I–VI vs 0) |
| TC, mmol/L | 5.44 | 5.08 | 5.17 | 5.43 | 0.78 | 0.38 | 5.46 | 5.03 | 5.19 | 5.43 | 0.82 | 0.33 | 5.49 | 5.07 | 5.17 | 5.42 | 0.92 | 0.32 |
| LDLC, mmol/L | 3.75 | 3.25 | 3.34 | 3.45 | 0.59 | 0.12 | 3.77 | 3.21 | 3.36 | 3.45 | 0.58 | 0.11 | 3.83 | 3.24 | 3.36 | 3.46 | 0.50 | 0.09 |
| HDLC, mmol/L | 1.28 | 1.29 | 1.28 | 1.31 | 0.80 | 0.87 | 1.28 | 1.29 | 1.27 | 1.33 | 0.64 | 0.88 | 1.25 | 1.30 | 1.26 | 1.34 | 0.47 | 0.62 |
| TG, mmol/L | 1.09 | 1.06 | 1.03 | 1.34 | 0.17 | 0.97 | 1.11 | 1.07 | 1.05 | 1.28 | 0.33 | 0.94 | 1.14 | 1.08 | 1.04 | 1.24 | 0.56 | 0.73 |
| TC/HDLC | 4.44 | 4.15 | 4.24 | 4.42 | 0.88 | 0.55 | 4.46 | 4.11 | 4.30 | 4.34 | 0.96 | 0.49 | 4.58 | 4.11 | 4.33 | 4.32 | 0.73 | 0.32 |
| LDLC/HDLC | 2.96 | 2.72 | 2.75 | 2.81 | 0.78 | 0.46 | 2.98 | 2.69 | 2.78 | 2.78 | 0.69 | 0.41 | 3.07 | 2.70 | 2.81 | 2.78 | 0.55 | 0.28 |
| Non-HDLC, mmol/L | 4.16 | 3.79 | 3.88 | 4.13 | 0.84 | 0.35 | 4.19 | 3.74 | 3.92 | 4.10 | 0.92 | 0.29 | 4.24 | 3.77 | 3.91 | 4.08 | 0.91 | 0.23 |

Abbreviations: HDLC = high-density lipoprotein cholesterol; LDLC = low-density lipoprotein cholesterol; TC = total cholesterol; TG = triglycerides.

[a] Model 1 was adjusted for age and sex. Model 2 was adjusted for age, sex, systolic blood pressure, fasting blood glucose, fasting insulin, body mass index, current smoking, regular exercise, and cerebrovascular disease. Model 3 was adjusted for age, sex, systolic blood pressure, fasting blood glucose, fasting insulin, body mass index, current smoking, regular exercise, cerebrovascular disease, and *APOE* ε4 carrier. Geometric mean of triglycerides is shown due to the skewed distribution.

another example that plaques and NFT are driven by very different factors.

Cholesterol may be associated with levels of the amyloid-precursor-protein metabolite Aβ, although the effects of cholesterol on Aβ metabolism, amyloid fibrillogenesis, and toxicity are not well understood and the results reported so far are controversial.[19,20] Aβ, apoE, cholesterol, and cholesterol oxidase have been shown to colocalize in the core of fibrillary plaques in transgenic mice models of AD,[21,22] which suggests that cholesterol and apoE are involved in fibrillar plaque formation. Previous studies have also found that levels of serum cholesterol, especially in the form of LDLC in patients with AD, were significantly higher when compared to age-matched controls.[23] A change in membrane properties, including stiffness and fluidity, has been suggested to influence activities of membrane-bound proteins and enzymes, including secretases. The high cholesterol content in lipid rafts, membrane regions where these enzymes are located, facilitates the clustering of the β and γ secretases with their substrates into an optimum configuration, thereby promoting the undesirable pathogenic cleavage of amyloid precursor protein.[24]

There are few previous studies that have investigated the association between hypercholesterolemia and AD-related pathology.[6,7] Of these, the Honolulu-Asia Aging Study was a population-based study which reported that the constituents of HDLC may play a role in the formation of AD pathology. The discrepancy between these and our results may reflect differences in study design. One difference is in the observation period between the evaluation of cholesterolemia and autopsy. Because the observation period in our study was relatively long (10–15 years) compared with the Honolulu-Asia Aging Study (<8 years), our study design might reduce the possibility of reverse causality; the presence of AD might affect the lifestyle of the subjects and their lipid profiles. Another retrospective study shows that serum hypercholesterolemia may be a risk factor for the development of AD amyloid pathology.[6] This study was not population-based and the increased risk is observed only among subjects younger than 55 years of age; however, significant association between serum cholesterol and the development of amyloid pathology is consistent with our findings.

Meanwhile, the relationship between cholesterol levels and clinical manifestation of dementia is less clear.[25] Epidemiology studies show controversial findings; high cholesterol levels in midlife may increase risk for subsequent dementia and AD[26–29] or low cholesterol levels in late life have been predictive of subsequent dementia.[30] Differences in study designs, length of observational periods, analytical

Table 4 **Multivariate-adjusted ORs and 95% CIs for presence of NPs (CERAD score 1–3 vs 0) according to lipid profile levels[a]**

| Quantiles of lipid profiles | Range | No. of subjects with NPs/total (%) | Model 1 | | Model 2 | | Model 3 | |
|---|---|---|---|---|---|---|---|---|
| | | | OR (95% CI) | p Value | OR (95% CI) | p Value | OR (95% CI) | p Value |
| **TC, mmol/L** | | | | | | | | |
| Q1 | ≤4.48 | 23/37 (62.2) | | | | | | |
| Q2 (vs Q1) | >4.48 and ≤5.20 | 23/37 (62.2) | 1.1 (0.4-3.1) | 0.93 | 0.9 (0.3-2.9) | 0.8302 | 1.1 (0.3-4.4) | 0.93 |
| Q3 (vs Q1) | >5.20 and ≤5.80 | 23/37 (62.2) | 1.0 (0.3-3.1) | 0.96 | 0.7 (0.2-2.6) | 0.62 | 0.7 (0.2-3.1) | 0.65 |
| Q4 (vs Q1) | >5.80 | 31/36 (86.1) | 6.8 (1.8-25.4) | 0.005 | 8.2 (1.9-35.2) | 0.004 | 23.1 (3.8-141.6) | 0.0007 |
| Q4 (vs Q1–3) | | | 6.6 (2.1-20.5) | 0.001 | 9.6 (2.7-34.1) | 0.0005 | 24.8 (4.7-130.5) | 0.0002 |
| **LDLC, mmol/L** | | | | | | | | |
| Q1 | ≤2.75 | 22/37 (59.5) | | | | | | |
| Q2 (vs Q1) | >2.75 and ≤3.35 | 24/36 (66.7) | 1.6 (0.5-5.2) | 0.39 | 1.1 (0.3-3.9) | 0.87 | 1.0 (0.2-4.0) | 0.97 |
| Q3 (vs Q1) | >3.35 and ≤4.02 | 23/37 (62.2) | 1.2 (0.4-3.6) | 0.75 | 1.1 (0.3-3.8) | 0.86 | 1.5 (0.4-6.0) | 0.61 |
| Q4 (vs Q1) | >4.02 | 30/35 (85.7) | 7.5 (1.9-29.0) | 0.004 | 8.1 (1.9-34.0) | 0.005 | 13.5 (2.5-73.1) | 0.003 |
| Q4 (vs Q1–3) | | | 5.8 (1.8-18.4) | 0.003 | 7.5 (2.2-25.3) | 0.001 | 11.6 (2.7-49.4) | 0.0009 |
| **HDLC, mmol/L** | | | | | | | | |
| Q4 | >1.50 | 20/31 (64.5) | | | | | | |
| Q3 (vs Q4) | >1.27 and ≤1.50 | 24/38 (63.2) | 0.7 (0.2-2.1) | 0.49 | 0.7 (0.2-2.5) | 0.63 | 0.9 (0.2-3.8) | 0.94 |
| Q2 (vs Q4) | >1,04 and ≤1.27 | 25/41 (61.0) | 0.9 (0.3-2.7) | 0.86 | 1.0 (0.3-3.3) | 0.94 | 1.0 (0.2-3.8) | 0.95 |
| Q1 (vs Q4) | ≤1.04 | 31/37 (83.8) | 3.2 (0.9-11.5) | 0.07 | 2.8 (0.7-11.0) | 0.15 | 1.7 (0.4-7.8) | 0.49 |
| Q1 (vs Q2–4) | | | 3.8 (1.3-10.9) | 0.01 | 3.1 (1.1-9.2) | 0.04 | 1.8 (0.6-5.6) | 0.34 |
| **TG, mmol/L** | | | | | | | | |
| Q1 | ≤0.81 | 26/38 (68.4) | | | | | | |
| Q2 (vs Q1) | >0.81 and ≤1.11 | 25/36 (69.4) | 0.9 (0.3-2.8) | 0.88 | 1.0 (0.3-3.4) | >0.99 | 0.9 (0.2-3.3) | 0.87 |
| Q3 (vs Q1) | >1.11 and ≤1.56 | 22/38 (57.9) | 0.5 (0.2-1.5) | 0.21 | 0.5 (0.2-1.7) | 0.28 | 0.6 (0.2-2.1) | 0.40 |
| Q4 (vs Q1) | >1.56 | 27/35 (77.1) | 2.7 (0.8-8.9) | 0.11 | 3.1 (0.8-12.4) | 0.10 | 2.7 (0.6-12.2) | 0.19 |
| Q4 (vs Q1–3) | | | 3.5 (1.2-9.6) | 0.02 | 4.0 (1.3-12.8) | 0.02 | 3.5 (1.0-12.3) | 0.05 |
| **TC/HDLC** | | | | | | | | |
| Q1 | ≤3.32 | 21/37 (56.8) | | | | | | |
| Q2 (vs Q1) | >3.32 and ≤4.09 | 23/37 (62.2) | 1.1 (0.4-3.2) | 0.86 | 1.4 (0.4-4.4) | 0.62 | 1.2 (0.3-4.4) | 0.77 |
| Q3 (vs Q1) | >4.09 and ≤5.10 | 24/38 (63.2) | 1.8 (0.6-5.5) | 0.27 | 2.6 (0.7-9.2) | 0.14 | 1.8 (0.4-7.7) | 0.41 |
| Q4 (vs Q1) | >5.10 | 32/35 (91.4) | 13.0 (2.8-59.9) | 0.001 | 18.1 (3.1-105.5) | 0.001 | 19.7 (2.6-149.4) | 0.004 |
| Q4 (vs Q1–3) | | | 9.7 (2.5-37.1) | 0.0009 | 9.7 (2.3-40.1) | 0.002 | 13.1 (2.5-68.6) | 0.002 |
| **LDLC/HDLC** | | | | | | | | |
| Q1 | ≤2.00 | 24/38 (63.2) | | | | | | |
| Q2 (vs Q1) | >2.00 and ≤2.64 | 23/35 (65.7) | 1.1 (0.4-3.1) | 0.90 | 1.0 (0.3-3.3) | >0.99 | 1.0 (0.3-3.5) | 0.96 |
| Q3 (vs Q1) | >2.64 and ≤3.48 | 21/37 (56.8) | 1.1 (0.4-3.2) | 0.92 | 1.3 (0.4-4.3) | 0.68 | 1.2 (0.3-4.9) | 0.75 |
| Q4 (vs Q1) | >3.48 | 31/35 (88.6) | 5.7 (1.4-23.0) | 0.01 | 6.9 (1.4-32.7) | 0.02 | 7.9 (1.2-50.5) | 0.03 |
| Q4 (vs Q1–3) | | | 5.5 (1.7-18.1) | 0.005 | 6.0 (1.7-21.8) | 0.007 | 7.0 (1.5-32.0) | 0.01 |
| **Non-HDLC, mmol/L** | | | | | | | | |
| Q1 | ≤3.29 | 23/38 (60.5) | | | | | | |
| Q2 (vs Q1) | >3.29 and ≤3.86 | 24/37 (64.9) | 1.0 (0.4-3.1) | 0.94 | 0.9 (0.3-3.0) | 0.82 | 0.7 (0.2-2.9) | 0.65 |
| Q3 (vs Q1) | >3.86 and ≤4.61 | 22/37 (59.5) | 1.0 (0.4-3.1) | 0.95 | 1.0 (0.3-3.3) | 0.95 | 0.7 (0.2-2.9) | 0.64 |
| Q4 (vs Q1) | >4.61 | 31/35 (88.6) | 8.5 (2.1-34.6) | 0.003 | 10.1 (2.1-48.2) | 0.004 | 13.1 (2.3-75.9) | 0.004 |
| Q4 (vs Q1–3) | | | 8.2 (2.4-28.2) | 0.0008 | 10.7 (2.8-40.5) | 0.0005 | 16.5 (3.5-77.6) | 0.0004 |

Abbreviations: CERAD = Consortium to Establish a Registry for Alzheimer's Disease; CI = confidence interval; HDLC = high-density lipoprotein cholesterol; LDLC = low-density lipoprotein cholesterol; NP = neuritic plaque; OR = odds ratio; TC = total cholesterol; TG = triglycerides.

[a] Model 1 was adjusted for age and sex. Model 2 was adjusted for age, sex, systolic blood pressure, fasting blood glucose, fasting insulin, body mass index, current smoking, cerebrovascular disease, and regular exercise. Model 3 was adjusted for age, sex, systolic blood pressure, fasting blood glucose, fasting insulin, body mass index, current smoking, regular exercise, cerebrovascular disease, and *APOE* ε4 carrier.

strategies, and the age at the occurrence of high cholesterol may influence observations.[31] Our study evaluated how cholesterol affects the neuropathologic process of AD; however, dyslipidemia might also affect mechanisms other than NP formation in the onset of dementia or AD, such as cell-membrane maintenance or synaptic function.

There are some limitations to our present study. First, the crude, semiquantitative evaluation of NPs (CERAD) and NFTs (Braak stage) could affect the results of the present study. Second, the medical history of dyslipidemia, such as disease duration, use of medication, and complications, were not considered in this study. Medication or change of lifestyle between the clinical examination and death might affect the lipid profiles during a follow-up period; therefore, the association between lipid profiles and AD pathology could be underestimated in this study.

Despite these limitations, our study has several strengths. The main advantage over other studies is the direct measurement of lipid profiles, such as TC, TG, and HDLC, more than a decade before subjects died. We included community-based subjects, who had detailed metabolic characterization at midlife based on comprehensive blood testing, and we systematically assessed AD pathology. Accordingly, the data included in this study are valuable for the examination of metabolic risk factors for AD pathology. In the Hisayama Study, both participation rate of clinical examinations and autopsy rate have remained at high levels. Therefore, our results could apply to other Japanese populations.

As part of the Hisayama Study, we have shown that dyslipidemia, in addition to insulin resistance, may be an independent risk factor for NP formation. Due to the long follow-up period, a number of other factors may have come into play. Nonetheless, our study clearly makes the point that lipid profiles may contribute directly or indirectly to plaque burden in the brain. Because a direct measurement of LDLC may be unreliable, and for the purpose of additional consideration of very low-density lipoprotein and intermediate density lipoprotein cholesterol, the values of non-HDLC might help to predict the development of NPs. Further studies are required to determine if there is a causal link between dyslipidemia and the development of NPs or other AD-related pathologies. In the future, adequate control of cholesterol, in addition to the control of diabetes, might contribute to a strategy for the prevention of AD.

## AUTHOR CONTRIBUTIONS

Dr. Matsuzaki: drafting/revising the manuscript, study concept or design, analysis or interpretation of data, acquisition of data, statistical analysis. Dr. Sasaki: drafting/revising the manuscript, study concept or design, analysis or interpretation of data, acquisition of data, obtaining funding. Dr. Hata: drafting/revising the manuscript, analysis or interpretation of data, acquisition of data, statistical analysis. Dr. Hirakawa: analysis or interpretation of data, acquisition of data. Dr. Fujimi: analysis or interpretation of data, acquisition of data. Dr. Ninomiya: drafting/revising the manuscript, acquisition of data. Dr. Suzuki: drafting/revising the manuscript, analysis or interpretation of data, contribution of vital reagents/tools/patients, acquisition of data. Dr. Kanba: analysis or interpretation of data, study supervision. Dr. Kiyohara: drafting/revising the manuscript, study concept or design, analysis or interpretation of data, contribution of vital reagents/tools/patients, acquisition of data, study supervision, obtaining funding. Dr. Iwaki: drafting/revising the manuscript, study concept or design, analysis or interpretation of data, acquisition of data, study supervision, obtaining funding.

## ACKNOWLEDGMENT

The authors thank S. Nagae and K. Sato for technical assistance.

## DISCLOSURE

Dr. Matsuzaki reports no disclosures. Dr. Sasaki receives research support from Grant-in-Aid for Scientific Research (C) from Japan Society for the Promotion of Science and Grant-in-Aid for Scientists from the Ministry of Health, Labour and Welfare, Japan. Dr. Hata, Dr. Hirakawa, Dr. Fujimi, Dr. Ninomiya, and Dr. Suzuki report no disclosures. Dr. Kanba serves on a scientific advisory board for Astellas Pharma Inc.; serves/has served on editorial advisory boards for *Molecular Psychiatry*, the *Journal of Neuroscience and Psychiatry*, the *Asian Journal of Psychiatry*, and the *Asia Pacific Journal of Psychiatry*; has received speaker honoraria from Janssen, Shanghai Tsumura Pharmaceuticals Co., Ltd., Ajinomoto Co., Inc., Yoshitomi Pharmaceutical Industries, Ltd., Meiji Seika Pharma Co., Ltd, Kyowa-Hakko, Dainippon Sumitomo Pharma Co., Ltd., Organon Pharmaceuticals, Otsuka Pharmaceutical Co., Ltd., Astellas Pharma Inc., Eli Lilly and Company, GlaxoSmithKline, Pfizer Inc, Asahi Kasei Kuraray Medical Co., Ltd., and Shionogi & Co., Ltd.; has served as consultant for Eli Lilly and Company, GlaxoSmithKline, Pfizer Inc, Mitsubishi Tanabe Pharma Corporation, Ono Pharmaceutical Co. Ltd., Astellas Pharma Inc., Asahi-kasei, Shionogi, and Otsuka Pharmaceutical Co., Ltd.; and receives/has received research support from has received research support from Eli Lilly and Company, GlaxoSmithKline, Pfizer Inc, Asahi Kasei Kuraray Medical Co., Ltd., Janssen, Shanghai Tsumura Pharmaceuticals Co., Ltd., Ajinomoto Co., Inc., Yoshitomi Pharmaceutical Industries, Ltd., Meiji Seika Pharma Co., Ltd, Kyowa Hakko Kirin Pharma, Inc., Dainippon Sumitomo Pharma Co., Ltd., Organon Pharmaceuticals, Otsuka Pharmaceutical Co., Ltd., Ono Pharmaceutical Co. Ltd., and Japanese Ministry of Education and of Health. Dr. Kiyohara receives research support from a Health and Labour Sciences Research Grant of the Ministry of Health, Labour and Welfare, Japan. Dr. Iwaki serves as an Associate Editor for *Brain Tumor Pathology* and on the editorial boards of *Neuropathology*, *Pathology-Research and Practice*, and *Pathology International*; and receives research support from a Grant-in-Aid for Scientific Research (B) from Japan Society for the Promotion of Science (JSPS).

*Received February 16, 2011. Accepted in final form May 23, 2011.*

## REFERENCES

1. Matsui Y, Tanizaki Y, Arima H, et al. Incidence and survival of dementia in a general population of Japanese elderly: the Hisayama Study. J Neurol Neurosurg Psychiatry 2009;80:366–370.
2. Sekita A, Ninomiya T, Tanizaki Y, et al. Trends in prevalence of Alzheimer's disease and vascular dementia in a Japanese community: the Hisayama Study. Acta Psychiatr Scand 2010;122:319–325.
3. Matsuzaki T, Sasaki K, Tanizaki Y, et al. Insulin resistance is associated with the pathology of Alzheimer disease: the Hisayama Study. Neurology 2010;75:764–770.
4. Peila R, Rodriguez BL, Launer LJ. Type 2 diabetes, APOE gene, and the risk for dementia and related pathologies:

The Honolulu-Asia Aging Study. Diabetes 2002;51:1256–1262.
5. Arvanitakis Z, Schneider JA, Wilson RS, et al. Diabetes is related to cerebral infarction but not to AD pathology in older persons. Neurology 2006;67:1960–1965.
6. Pappolla MA, Bryant-Thomas TK, Herbert D, et al. Mild hypercholesterolemia is an early risk factor for the development of Alzheimer amyloid pathology. Neurology 2003;61:199–205.
7. Launer LJ, White LR, Petrovitch H, Ross GW, Curb JD. Cholesterol and neuropathologic markers of AD: a population-based autopsy study. Neurology 2001;57:1447–1452.
8. Katsuki S. Epidemiological and clinicopathological study on cerebrovascular disease in Japan. Prog Brain Res 1966;21:64–89.
9. Ohmura T, Ueda K, Kiyohara Y, et al. Prevalence of type 2 (non-insulin-dependent) diabetes mellitus and impaired glucose tolerance in the Japanese general population: the Hisayama Study. Diabetologia 1993;36:1198–1203.
10. Fujimi K, Sasaki K, Noda K, et al. Clinicopathological outline of dementia with Lewy bodies applying the revised criteria: the Hisayama Study. Brain Pathol 2008;18:317–325.
11. Friedewald WT, Levy RI, Fredrickson DS. Estimation of the concentration of low-density lipoprotein cholesterol in plasma, without use of the preparative ultracentrifuge. Clin Chem 1972;18:499–502.
12. Mirra SS, Heyman A, McKeel D, et al. The Consortium to Establish a Registry for Alzheimer's Disease (CERAD): part II: standardization of the neuropathologic assessment of Alzheimer's disease. Neurology 1991;41:479–486.
13. Braak H, Braak E. Neuropathological stageing of Alzheimer-related changes. Acta Neuropathol 1991;82:239–259.
14. Braak H, Alafuzoff I, Arzberger T, Kretzschmar H, Del Tredici K. Staging of Alzheimer disease-associated neurofibrillary pathology using paraffin sections and immunocytochemistry. Acta Neuropathol 2006;112:389–404.
15. Brown MS, Goldstein JL. A receptor-mediated pathway for cholesterol homeostasis. Science 1986;232:34–47.
16. Saunders AM, Strittmatter WJ, Schmechel D, et al. Association of apolipoprotein E allele epsilon 4 with late-onset familial and sporadic Alzheimer's disease. Neurology 1993;43:1467–1472.
17. Ingelsson E, Schaefer EJ, Contois JH, et al. Clinical utility of different lipid measures for prediction of coronary heart disease in men and women. JAMA 2007;298:776–785.
18. Hardy J. Alzheimer's disease: the amyloid cascade hypothesis: an update and reappraisal. J Alzheimers Dis 2006;9:151–153.
19. Simons M, Keller P, De Strooper B, Beyreuther K, Dotti CG, Simons K. Cholesterol depletion inhibits the generation of beta-amyloid in hippocampal neurons. Proc Natl Acad Sci USA 1998;95:6460–6464.
20. Bodovitz S, Klein WL. Cholesterol modulates alpha-secretase cleavage of amyloid precursor protein. J Biol Chem 1996;271:4436–4440.
21. Hayashi H, Kimura N, Yamaguchi H, et al. A seed for Alzheimer amyloid in the brain. J Neurosci 2004;24:4894–4902.
22. Burns MP, Noble WJ, Olm V, et al. Co-localization of cholesterol, apolipoprotein E and fibrillar Abeta in amyloid plaques. Brain Res Mol Brain Res 2003;110:119–125.
23. Kuo YM, Emmerling MR, Bisgaier CL, et al. Elevated low-density lipoprotein in Alzheimer's disease correlates with brain abeta 1–42 levels. Biochem Biophys Res Commun 1998;252:711–715.
24. Wahrle S, Das P, Nyborg AC, et al. Cholesterol-dependent gamma-secretase activity in buoyant cholesterol-rich membrane microdomains. Neurobiol Dis 2002;9:11–23.
25. Anstey KJ, Lipnicki DM, Low LF. Cholesterol as a risk factor for dementia and cognitive decline: a systematic review of prospective studies with meta-analysis. Am J Geriatr Psychiatry 2008;16:343–354.
26. Notkola IL, Sulkava R, Pekkanen J, et al. Serum total cholesterol, apolipoprotein E epsilon 4 allele, and Alzheimer's disease. Neuroepidemiology 1998;17:14–20.
27. Kivipelto M, Helkala EL, Laakso MP, et al. Apolipoprotein E epsilon4 allele, elevated midlife total cholesterol level, and high midlife systolic blood pressure are independent risk factors for late-life Alzheimer disease. Ann Intern Med 2002;137:149–155.
28. Whitmer RA, Sidney S, Selby J, Johnston SC, Yaffe K. Midlife cardiovascular risk factors and risk of dementia in late life. Neurology 2005;64:277–281.
29. Solomon A, Kivipelto M, Wolozin B, Zhou J, Whitmer RA. Midlife serum cholesterol and increased risk of Alzheimer's and vascular dementia three decades later. Dement Geriatr Cogn Disord 2009;28:75–80.
30. Mielke MM, Zandi PP, Sjogren M, et al. High total cholesterol levels in late life associated with a reduced risk of dementia. Neurology 2005;64:1689–1695.
31. Mielke MM, Zandi PP, Shao H, et al. The 32-year relationship between cholesterol and dementia from midlife to late life. Neurology 2010;75:1888–1895.

Schizophrenia Research 129 (2011) 172–182

Contents lists available at ScienceDirect

Schizophrenia Research

journal homepage: www.elsevier.com/locate/schres

# Aripiprazole inhibits superoxide generation from phorbol-myristate-acetate (PMA)-stimulated microglia in vitro: Implication for antioxidative psychotropic actions via microglia

Takahiro A. Kato [a,b,*], Akira Monji [a,*], Keiji Yasukawa [b,c], Yoshito Mizoguchi [a], Hideki Horikawa [a], Yoshihiro Seki [a], Sadayuki Hashioka [a], Youn-Hee Han [c,d], Mina Kasai [a], Noriyuki Sonoda [b,e], Eiichi Hirata [b,e], Yasutaka Maeda [b,e], Toyoshi Inoguchi [b,e], Hideo Utsumi [b], Shigenobu Kanba [a]

[a] Department of Neuropsychiatry, Graduate School of Medical Sciences, Kyushu University, Maidashi 3-1-1, Higashi-ku, Fukuoka 812-8582, Japan
[b] Innovation Center for Medical Redox Navigation, Kyushu University, Maidashi 3-1-1, Higashi-ku, Fukuoka 812-8582, Japan
[c] Department of Chemo-Pharmaceutical Sciences, Graduate School of Pharmaceutical Sciences, Kyushu University, 3-1-1 Maidashi Higashi-ku, Fukuoka 812-8582, Japan
[d] Department of Civil and Environmental Engineering, Tohoku Gakuin University, 1-13-1 Chou, Tagajo, 985-8537, Japan
[e] Department of Internal Medicine and Bioregulatory Science, Graduate School of Medical Sciences, Kyushu University, Maidashi 3-1-1, Higashi-ku, Fukuoka 812-8582, Japan

ARTICLE INFO

*Article history:*
Received 1 October 2010
Received in revised form 20 March 2011
Accepted 21 March 2011
Available online 15 April 2011

*Keywords:*
Microglia
Schizophrenia
Oxidative stress
Antipsychotics
Superoxide
NADPH oxidase

ABSTRACT

Altered antioxidant status has been implicated in schizophrenia. Microglia, major sources of free radicals such as superoxide ($\bullet O_2^-$), play crucial roles in various brain pathologies. Recent postmortem and imaging studies have indicated microglial activation in the brain of schizophrenic patients. We previously demonstrated that atypical antipsychotics including aripiprazole significantly inhibited the release of nitric oxide and proinflammatory cytokines from interferon-γ-stimulated microglia in vitro. Antioxidative effects of antipsychotics via modulating microglial superoxide generation have never been reported. Therefore, we herein investigated the effects of antipsychotics on the $\bullet O_2^-$ generation from phorbol-myristate-acetate (PMA)-stimulated rodent microglia by the electron spin resonance (ESR) spectroscopy and also examined the intracellular mechanism by intracellular $Ca^{2+}$ imaging and immunostaining. Neuronal damage induced by microglial activation was also investigated by the co-culture experiment.

Among various antipsychotics, only aripiprazole inhibited the $\bullet O_2^-$ generation from PMA-stimulated microglia. Aripiprazole proved to inhibit the $\bullet O_2^-$ generation through the cascade of protein kinase C (PKC) activation, intracellular $Ca^{2+}$ regulation and NADPH oxidase activation via cytosolic $p47^{phox}$ translocation to the plasma/phagosomal membranes. Formation of neuritic beading, induced by PMA-stimulated microglia, was attenuated by pretreatment of aripiprazole.

D2R antagonism has long been considered as the primary therapeutic action for schizophrenia. Aripiprazole with D2R partial agonism is effective like other antipsychotics with fewer side effects, while aripiprazole's therapeutic mechanism itself remains unclear. Our results imply that aripiprazole may have psychotropic effects by reducing the microglial oxidative reactions and following neuronal reactions, which puts forward a novel therapeutic hypothesis in schizophrenia research.



## 1. Introduction

Altered antioxidant status has recently been implicated in schizophrenia with increasing number of clinical evidence measuring biochemical components for detoxification of reactive oxygen species (ROS) such as glutathione (GSH) and superoxide dismutase (SOD) (Do et al., 2009; Ng et al., 2008; Yao et al., 2001; Zhang et al., 2009a). A recent postmortem study and a cerebral spectroscopic study indicated a positive relationship between oxidative stress and schizophrenia (Treasaden and Puri, 2008; Wang et al., 2009). Overproduction of neutrophil ROS has reported to correlate with negative symptoms in schizophrenia (Sirota et al., 2003). Ketamine, which can lead to a syndrome indistinguishable from schizophrenia, has recently been

*Abbreviations:* DMSO, dimethyl sulfoxide; DPI, diphenylene iodonium; D2R, dopamine D2 receptor; ESR, electron spin resonance; GSH, glutathione; GM-CSF, granulocyte macrophage colony stimulating factor; $[Ca^{2+}]i$, intracellular $Ca^{2+}$ concentration; NAC, N-Acetyl cysteine; NGF, nerve growth factor; NO, nitric oxide; PKC, protein kinase C; ROS, reactive oxygen species; $\bullet O_2^-$, superoxide; SOD, superoxide dismutase; TNF-α, tumor necrosis factor-α.

* Corresponding authors at: Department of Neuropsychiatry, Graduate School of Medical Sciences, Kyushu University, Maidashi 3-1-1, Higashi-ku, Fukuoka 812-8582, Japan. Tel.: +81 92 642 5627; fax: +81 92 642 5644.
*E-mail addresses:* takahiro@npsych.med.kyushu-u.ac.jp (T.A. Kato), amonji@hf.rim.or.jp (A. Monji).

0920-9964/$ – see front matter © 2011 Elsevier B.V. All rights reserved.
doi:10.1016/j.schres.2011.03.019

reported to induce a persistent increase in brain superoxide radicals due to activation of NADPH oxidase (Behrens et al., 2007). On the other hand, N-Acetyl cysteine (NAC), a glutathione precursor, has recently been reported to be effective for augmentation therapy of chronic schizophrenia and to improve impaired mismatch negativity in schizophrenic patients (Berk et al., 2008; Lavoie et al., 2008). More recently, the serum levels of SOD in chronic patients with schizophrenia are associated with psychopathology and response to antipsychotics (Zhang et al., 2009b). These findings suggest that regulation of oxidative stress may be related to the pathophysiology and therapeutic mechanism of schizophrenia.

Microglia, major sources of free radicals such as superoxide ($\bullet O_2^-$) and nitric oxide (NO) in the CNS, play a crucial role in variety of brain pathologies (Block and Hong, 2005; Block et al., 2007; Hanisch and Kettenmann, 2007). The pathophysiology of schizophrenia remains unclear, while recent postmortem brain studies using class II human leucocyte antigen (HLA-DR) have revealed microglial activation in the brains of schizophrenic patients (Radewicz et al., 2000; Steiner et al., 2008). Positron emission computed tomography (PET) studies with specific ligand of the peripheral benzodiazepine-binding sites (PBBS), have indicated that activated microglia may be present in schizophrenic patients (Doorduin et al., 2009; Takano et al., 2010; van Berckel et al., 2008). There is accumulated evidence that gene–environmental interaction via various factors such as virus infections and social stress leads to development of schizophrenia (Dalman et al., 2008; Jia et al., 2010; Mortensen et al., 2010; van Winkel et al., 2008). Microglia is one of the key players in brain damages induced by virus infections in the CNS (Block et al., 2007). One recent experiment suggested that social stress – isolation – induces NADPH oxidase activation via microglia in rat brain (Schiavone et al., 2009). These reports indicate that microglia may play an important role in gene–environmental interaction associated with schizophrenia (Sawa et al., 2004; Seshadri et al., 2010).

Dopamine system dysfunction has been for long time hypothesized in the pathology of schizophrenia, and dopamine D2 receptor (D2R) antagonism against dopamine neurons has been considered as the primary therapeutic target for schizophrenia (Kapur and Mamo, 2003; Miyamoto et al., 2005). On the other hand, aripiprazole is a novel unique atypical antipsychotic drug, which is a high-affinity D2R partial agonist (Burris et al., 2002; Shapiro et al., 2003). In spite of its different pharmacological profile, aripiprazole is effective against the positive and negative symptoms of patients with schizophrenia like other antipsychotics with fewer side effects (Leucht et al., 2009; Potkin et al., 2003).

We recently demonstrated that not only atypical antipsychotics with D2R antagonism but also aripiprazole with D2R partial agonism significantly inhibited the release of NO and proinflammatory cytokines such as tumor necrosis factor (TNF)-α on interferon-γ-stimulated microglia in vitro (Bian et al., 2008; Kato et al., 2008; Kato et al., 2007). Therapeutic benefits on psychotic symptoms have been demonstrated by COX-2 inhibitor and minocycline, both of which have proved to inhibit microglial activation (Akhondzadeh et al., 2007; Miyaoka et al., 2008; Muller et al., 2010). Summing up the above-mentioned evidence, we hypothesis that microglia may play a key role in the pathophysiology of schizophrenia by producing free radicals and cytokines in the CNS, and that microglial regulation may be a novel therapeutic target for schizophrenia (Monji et al., 2009).

To the best of our knowledge, antioxidative effects of antipsychotics via modulating microglial superoxide generation have never been reported. Phorbol-myristate-acetate (PMA), a typical activator of protein kinase C (PKC), induces $\bullet O_2^-$ from microglia with the elevation of intracellular calcium (Colton et al., 1992; Sankarapandi et al., 1998; Yoo et al., 1996). PKC has recently been indicated to be associated with stress-related illness and psychiatric disorders (Chen et al., 2009; Hains et al., 2009). Therefore, in the present study, we investigated the effects of various antipsychotics on the generation of $\bullet O_2^-$ from PMA-stimulated microglia by the electron spin resonance (ESR) spectroscopy and also examined the intracellular mechanism by intracellular $Ca^{2+}$ imaging and immunostaining. Neuronal damage induced by microglial activation was also investigated by co-culture experiment.

## 2. Materials and methods

### 2.1. Chemicals and reagents

PMA was purchased from Biomol International (Plymouth Meeting, PA, USA). LPS, haloperidol, clozapine, a D2R full agonist; quinpirole, NADPH oxidase inhibitors; diphenylene iodonium (DPI) and apocynin, and a spin trap; DEPMPO were purchased from Sigma Chemicals (St. Louis, MO, USA). SOD, catalase, xanthine, and xanthine oxidase were purchased from Wako Pure Chemical Industries (Osaka, Japan). Recombinant mouse GM-CSF was purchased from R&D systems (Minneapolis, MN, USA). WST-8 was purchased from Dojindo Molecular Technologies (Kumamoto, Japan). Atypical antipsychotics were generously provided by each manufacturer; aripiprazole from Otsuka Pharmaceutical Co., Ltd. (Tokyo, Japan), risperidone from Janssen Pharmaceutica NV (Beerse, Belgium), and olanzapine from Eli Lilly and Co. (Indianapolis, IN, USA). Antipsychotics were dissolved initially into 20 mM with dimethyl sulfoxide (DMSO) and then were diluted into final concentration for each experiment. The final concentrations of antipsychotics were not over 10 μM. All antipsychotics and DMSO at the highest concentration (0.05%) were confirmed not to be toxic to microglial cells in our previous reports (Kato et al., 2007, 2008).

### 2.2. Cell cultures

All experimental procedures were conducted in accordance with the Standard Guidelines for Animal Experiments of Kyushu University. Rat primary microglial cells were cultured as previously described (Kato et al., 2008; Seki et al., 2010). Briefly, primary mixed cells were prepared from the whole brain of the 3-day-postnatal Sprague–Dawley rats, using Cell Strainer (BD Falcon, Franklin Lakes, NJ). Primary rat microglial cells were selected after attachment to Aclar film (Nisshin EM, Tokyo, Japan) for 2 h in Dulbecco's Modified Eagle's Medium supplemented with 10% fetal bovine serum (10% FBS/DMEM). Aclar films were slightly washed by PBS and then transferred to fresh 10% FBS/DMEM, and the fresh microglia was expanded for 1–2 days. The purity of the isolated microglia was assessed by immunocytochemical staining for microglial marker, Iba-1, and >99% of cells were stained positively. Murine microglial 6-3 cells, which was established from neonatal C57BL/6J(H-2b) mice using a non-enzymatic and non-virus-transformed procedure and which closely resemble primary cultured microglia (Kanzawa et al., 2000; Sawada et al., 1998), were cultured as previously described (Bian et al., 2008; Kato et al., 2007). The rat pheochromocytoma PC12 cells were cultured as previously described (Bian et al., 2008). Briefly, the 6-3 cells and PC12 cells were cultured in Eagle's minimal essential medium, 0.3% $NaHCO_3$, 2 mM glutamine, 0.2% glucose, 10 g/mL insulin and 10% fetal calf serum, and then were maintained at 37 °C in a 5% $CO_2$ and 95% air atmosphere.

### 2.3. Measurements of superoxide production

#### 2.3.1. Electron spin resonance (ESR) spectroscopy

ESR, together with the spin-trapping agent DEPMPO was employed to accurately detect the production of $\bullet O_2^-$ from PMA-stimulated microglia. We previously described the detail methodology of the ESR (Hashioka et al., 2007a, 2007b). Briefly, the 6-3 cells were cultured on 12-well tissue plates at the density of $1.6 \times 10^6$ cells in 400 mL of serum-free medium per well. The 6-3 cells were incubated with 400 ng/mL PMA for 30 min in both the presence and absence of pretreatment of the antipsychotics for 5 h at 37 °C before beginning the detection of ESR spectra. Cell suspensions ($4 \times 10^6$ cells/

mL) in the culture medium containing 25 mM DEPMPO were transferred to a standard cell capillary, and the ESR measurements were performed at room temperature right after the incubation. The ESR spectra were obtained using a JES-RE1X ESR spectrometer (JEOL, Japan). The setting conditions of the instrument were as follows: magnetic field = 336.7 + 7.5 mT, modulation amplitude = 2000, modulation width = 0.1 mT, modulation frequency = 100 kHz, time constant = 0.1 s, microwave power = 10 mW, microwave frequency = 9430 MHz, and sweep time = 2 min.

ESR was also applied to the rat primary microglial cells. The cells were cultured on 12-well tissue plates at a much lower density of $1.6 \times 10^4$ cells in 400 mL of serum-free culture medium per well due to the difficulty in collecting these cells.

*2.3.2. Nitro blue tetrazolium (NBT) assay*

The quantification of $\bullet O_2^-$ production in microglial cells was performed with modification of Nitro blue tetrazolium (NBT) assay as previously reported (Choi et al., 2006; Tan and Berridge, 2000). As a water-soluble formazan dye, we used the WST-8 (2-(2-methoxy-4-nitrophenyl)-3-(4-nitrophenyl)-5-(2,4-disulfophenyl)-2H-tetrazolium monosodium salt; Dojindo, Kumamoto, Japan). Briefly, microglial cells grown on 96-well culture plates ($5 \times 10^3$ cells per well) were pre-incubated in the presence and absence of aripiprazole for 5 h and then the medium was changed to 50 μL chelated medium both in the presence and absence of 50 U/mL SOD at 37 °C. After 30 min of incubation with PMA (400 ng/mL), the supernatants were mixed with 5 μL WST-8 solution. The absorbance was read at 450 nm using a plate reader (Labsystems Multiscan MS). The comparative volumes of $\bullet O_2^-$ production were determined by the difference between the absorbance with SOD and that without SOD.

*2.4. Spin trapping in xanthine/xanthine oxidase system*

Xanthine oxidase (0.1 U/mL) was incubated with 0.4 mM xanthine in phosphate-buffer (PB) containing 2 mM DTPA and 20 mM DEPMPO in the presence and absence of aripiprazole. Xanthine oxidase was added last to the mixture to start the reaction. The ESR spectra were recorded at room temperature on a JES-RE1X ESR spectrometer. The setting conditions of the instrument were as follows: magnetic field = 336.7 + 7.5 mT, modulation amplitude = 500, modulation width = 0.1 mT, modulation frequency = 100 kHz, time constant = 0.03 s, microwave power = 10 mW, microwave frequency = 9430 MHz and sweep time = 2 min.

*2.5. Intracellular $Ca^{2+}$ imaging*

The experiments were performed in the external standard solution (in mM: 150 NaCl, 5 KCl, 2 $CaCl_2$, 1 $MgCl_2$, 10 glucose and 10 HEPES, pH 7.4 with Tris-OH) at room temperature as we reported previously (Kato et al., 2008; Mizoguchi et al., 2003, 2009). Intracellular $Ca^{2+}$ concentration ($[Ca^{2+}]i$) in response to PMA application was monitored using fura-2 AM (acetoxymethyl ester) (Grynkiewicz et al., 1985) in rat primary microglial cells. The cells plated on glass-base dish were loaded with 5 μM fura-2 AM (Dojindo, Kumamoto, Japan) for 20 min and washed three times with HEPES buffer before the measurement. During the measurement, while using an inverted microscope (20×; Olympus IX70-22FL, Olympus Co. Tokyo, Japan), external HEPES buffer was constantly perfused (10 mL/min). For fura-2 excitation, the cells were illuminated with two alternating wavelengths, 340 and 380 nm using a computerized system. The emitted light was collected at 510 nm using a cooled CCD camera (C4742-95ER, Hamamatsu Photonics, Hamamatsu, Japan) and images were stored every 5 s. These series of sequential data were analyzed using the AquaCosmos software package (Hamamatsu photonics, Hamamatsu, Japan). The $[Ca^{2+}]i$ was calculated from the ratio (R) of fluorescence recorded at 340 and 380 nm excitation wavelengths for each pixel within a cell boundary (AquaCosmos software). Calibrations (conversion of R340/380 values into calcium concentrations) were performed as described previously (Grynkiewicz et al., 1985). Basal $[Ca^{2+}]i$ was determined from the initial 10 images of each cell recording. A $[Ca^{2+}]i$ signal was defined as an increase in R 340/380 with clear time correlation to the application of PMA.

Increase of $[Ca^{2+}]i$ in response to PMA application was calculated as difference between basal $[Ca^{2+}]i$ and highest $[Ca^{2+}]i$ during the treatment of PMA. All data presented were obtained from at least five dishes and three different cell preparations.

*2.6. Morphology and immunofluorescence*

NADPH oxidase activation via cytosolic $p47^{phox}$ protein translocation was investigated as previously described (Qian et al., 2008). The 6-3 cells were seeded in non-coated 6-well plates at $5 \times 10^3$ cells/well. They were incubated in both the absence and presence of aripiprazole, diphenylene iodonium (DPI) or apocynin for 5 h respectively, and then treated with 400 ng/mL PMA for 30 min. After being rinsed twice in 0.1 M Hepes/KOH, cells were fixed with 4% paraformaldehyde for 10 min, and then rinsed with 0.1 M Hepes/KOH for 10 min. The morphological changes of the cells were examined under phase contrast microscopy (Nikon, Tokyo, Japan). Indirect immunofluorescence was performed using the following antibodies: goat anti-$p47^{phox}$ polyclonal antibody which recognized $p47^{phox}$, a cytosolic, regulatory subunit of NADPH oxidase (1:100 dilution; Abcam, Cambridge, MA, USA) and rabbit anti-Iba-1 polyclonal antibody (1:400; Wako Pure Chemical Industries Ltd, Osaka, Japan). Cells were incubated in primary antibodies diluted in PBS containing 5% normal horse serum at 4 °C overnight. After rinsing twice with PBS for 5 min, anti-goat rhodamine-conjugated secondary antibody (Southern Biotech, Birmingham, AL, USA) and anti-rabbit fluorescein isothiocyanate (FITC)-conjugated secondary antibody (Southern Biotech, Birmingham, AL, USA) were used for detection. Fluorescent images were captured with fluorescence microscope (OLYMPUS BX50; Olympus Co. Ltd, Tokyo, Japan).

*2.7. Co-culture experiment with microglial and neuronal cell lines*

The PC12 cells were plated on 24-well tissue culture plates at a density of $2 \times 10^3$ cells per 1 mL per well and were then incubated in the presence of 20 ng/mL nerve growth factor (NGF) at 37 °C for 7–10 days enough to develop neuritic formation. The 6-3 microglial cells were plated on Tissue Culture Inserts for 24-well plates (Greiner Bio-One GmbH, Frickenhausen, Germany) at a density of $1 \times 10^5$ cells per 200 μL per well and were then pre-incubated in the presence of DMSO (0.05%) or aripiprazole (10 μM) for 5 h and then each Tissue Culture Inserts was placed on the 24-well tissue culture plate with PC12 cells, respectively. After 2 h co-incubation with 400 ng/mL PMA, Tissue Culture Inserts were removed from the 24-well plates with PC12 cells. Neuritic beading formations of PC12 cells were observed and assessed under a phase-contrast microscope as previously reported (Park et al., 1996; Takeuchi et al., 2005). More than 100 neurons in duplicate wells were assessed blindly in three independent trials. The ratio of the numbers of neuritic beading (beads) per one neuronal cell was calculated.

*2.8. Statistics*

Data were expressed as the means ± SEM and analyzed by a one-way analysis of variance (ANOVA) followed by Tukey's post hoc test. The significance was established at a level of $p<0.05$. All the data of each group were confirmed to be normally distributed by the Shapiro–Wilk test ($p>0.05$).

## 3. Results

### 3.1. Effects of the antipsychotics on the $\cdot O_2^-$ production by PMA-stimulated microglia

First of all, we directly measured the generation of $\cdot O_2^-$ associated with PMA-stimulated murine 6-3 microglia by ESR spectroscopy with a spin trap DEPMPO. In the preparations of non-stimulated microglia (Fig. 1A), no signals were obtained. Microglial cells stimulated by 400 ng/mL PMA in the presence of DEPMPO showed prominent signals whose spectra consisted of a linear combination of a characteristic 12-line spectrum corresponding to $\cdot O_2^-$ spin adduct DEPMPO–OOH and an 8-line spectrum corresponding to OH spin adduct DEPMPO–OH (Fig. 1B). Computer simulation confirmed DEPMPO–OOH with hyper-fine splittings $a_N = 13.15$ G, $a^b_H = 10{:}59$ G, $a_p = 49.73$ G, $a^g_H = 0{:}72$ G and DEPMPO–OH with hyper-fine splittings $a_N = 12.43$ G, $a_H = 13.49$ G, $a_p = 50.39$ G. These values are consistent with those described previously (Sankarapandi et al., 1998). Previously, we had demonstrated that the spin adducts originated from $\cdot O_2^-$ radical, but not $\cdot OH-$ radical, which is derived from $H_2O_2$ (Hashioka et al., 2007b). In the present study, the effects of various types of antipsychotics on the generation of $\cdot O_2^-$ from PMA-stimulated microglia were evaluated. Pretreatment with aripiprazole, a partial D2R agonist, for 5 h considerably inhibited the signal intensity of the $\cdot O_2^-$ adduct (Fig. 1C), while other antipsychotics with D2R antagonism including haloperidol, olanzapine, clozapine and risperidone did not have any inhibitory effect on the signal intensity of the $\cdot O_2^-$ adduct (Fig. 1D–G). In order to confirm whether the inhibitory effect of aripiprazole was due to D2R agonism or not, the effect of quinpirole which is a D2R full agonist was evaluated. Quinpirole did not have any inhibitory effect on the signal intensity of the $\cdot O_2^-$ adduct (Fig. 1H). These results thus suggested that the inhibitory effects of aripiprazole on the generation of $\cdot O_2^-$ from PMA-stimulated microglia were independent of the effects of aripiprazole on D2R. In addition, we also prepared rat primary microglial cells for ESR to confirm the relevance of our results in the 6-3 cells. In the case of PMA-stimulated rat primary microglial cells, the $\cdot O_2^-$ like adduct was measured despite a very low signal intensity due to much smaller quantity of the rat primary microglial cells ($1.6 \times 10^4$) than that of the 6-3 cells ($1.6 \times 10^6$) (Fig. 2B). Aripiprazole considerably reduced the signal intensity of the above-mentioned $\cdot O_2^-$ like adduct (Fig. 2C). These results suggest that the inhibitory effects of aripiprazole on microglial activation were not limited to the 6-3 microglia. To confirm whether or not aripiprazole per se scavenges $\cdot O_2^-$, we measured the $\cdot O_2^-$ production in xanthine/xanthine oxidase system in both the presence and absence of aripiprazole by ESR monitoring with a spin trap DEPMPO. Fig. 3A shows typical ESR spectra consisting of DEPMPO–OOH and DEPMPO–OH in xanthine/xanthine oxidase system. The formation of these spin adducts via trapping $\cdot O_2^-$ was confirmed by our previous report (Hashioka et al., 2007b). The ESR spectra in the presence of aripiprazole (Fig. 3B) proved to be essentially the same as those shown in Fig. 3A, thus indicating that aripiprazole does not have scavenging effect on $\cdot O_2^-$. Similarly, other antipsychotics did not show any scavenging effect of $\cdot O_2^-$ (data not shown).

Since assays of free-radical production in cells are notoriously capricious (Abramov et al., 2005), in order to reinforce the ESR evidence above, we also quantified $\cdot O_2^-$ generation by the NBT assay. We observed that application of PMA significantly induced $\cdot O_2^-$ release from both the rat primary microglial cells (Fig. 4A) and the 6-3 microglial cells (Fig. 4B). Pretreatment with aripiprazole for 5 h significantly inhibited the $\cdot O_2^-$ release from PMA-stimulated microglial cells in comparison to the positive control, however, pretreatment of haloperidol and quinpirole did not have any inhibitory effects at all (Fig. 4B). In addition, we confirmed that 2 h-pretreatment of aripiprazole also inhibited the $\cdot O_2^-$ release dose-dependently (Fig. 4C). These results thus confirmed the relevance of the ESR results.

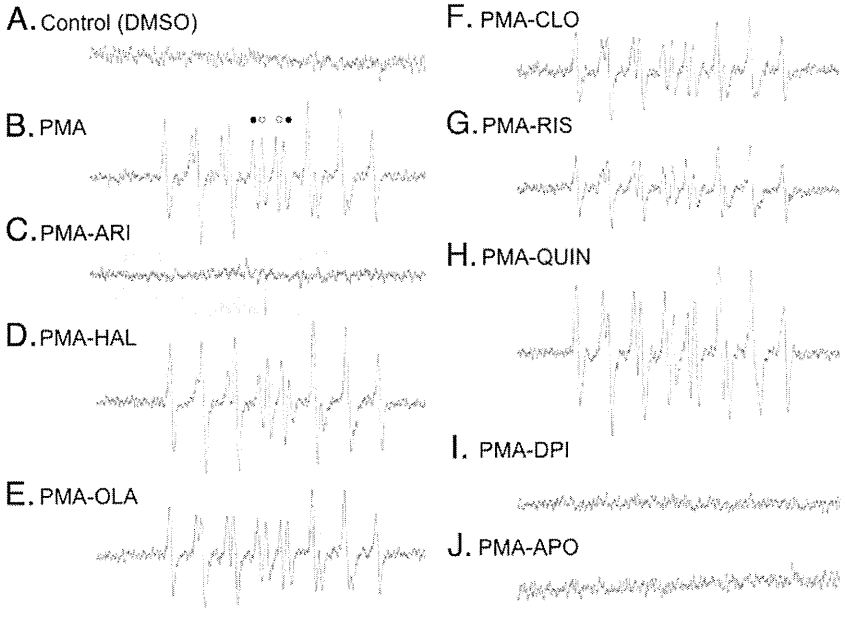


**Fig. 1.** Detection of $\cdot O_2^-$ generation by PMA-stimulated 6-3 microglial cells using ESR spin trap technique with DEPMPO. Murine 6-3 microglial cells ($4 \times 10^6$/mL) were prepared and incubated with PMA (400 ng/mL) for 30 min at 37 °C with and without pretreatment of antipsychotics for 5 h. The ESR spectra were then recorded in the presence of 25 mM DEPMPO at room temperature. (A) ESR spectra of DEPMPO adducts obtained from non-stimulated microglia. (B) ESR spectra of DEPMPO adducts obtained from PMA-stimulated microglia. Open and closed circles represent measured signal peaks of DEPMPO–OH and DEPMPO–OOH adducts, respectively. (C) ESR spectra of DEPMPO adducts obtained from microglia stimulated by PMA (400 ng/mL) after a 5 h pretreatment with aripiprazole (10 μM). (D) The same as (C) but with haloperidol (10 μM). (E) The same as (C) but with olanzapine (10 μM). (F) The same as (C) but with clozapine (10 μM). (G) The same as (C) but with risperidone (10 μM). (H) The same as (C) but with quinpirole (10 μM). (I) The same as (C) but with DPI (10 μM). (J) The same as (C) but with apocynin (1 μM).

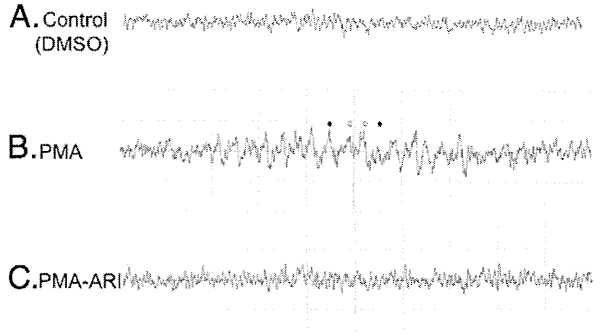


**Fig. 2.** Detection of $\cdot O_2^-$ generation by PMA-activated rat primary microglial cells using ESR spin trap technique with DEPMPO. Rat primary microglial cells ($4\times10^4$/mL) were prepared and incubated with PMA (400 ng/mL) for 30 min at 37 °C with and without pretreatment of aripiprazole for 5 h. The ESR spectra were then recorded in the presence of 25 mM DEPMPO at room temperature. (A) ESR spectra of DEPMPO adducts obtained from non-stimulated microglia. (B) ESR spectra of DEPMPO adducts obtained from PMA-stimulated microglia. Open and closed circles represent measured signal peaks of DEPMPO–OH and DEPMPO–OOH adducts, respectively. (C) ESR spectra of DEPMPO adducts obtained from microglia stimulated by PMA (400 ng/mL) after a 5 h pretreatment with aripiprazole (10 μM).

### *3.2. Aripiprazole inhibits PMA-induced translocation of NADPH oxidase cytosolic subunit of PHOX p47$^{phox}$ to the plasma/phagosomal membranes*

In the ESR experiments, not only aripiprazole but also NADPH oxidase inhibitors (diphenylene iodonium (DPI) and apocynin) proved to have a considerable inhibitory effect on PMA-induced $\cdot O_2^-$ generation from the murine microglial cells (Fig. 1I and J). Therefore, our results suggest that the $\cdot O_2^-$ generation in the microglial cells depends on NADPH oxidase pathway as previously reported (Sankarapandi et al., 1998). Inhibitory process of NADPH oxidase is reported to be different between DPI and apocynin: apocynin inhibits the translocation of subunits such as p47 and p67 in cytosol, while DPI acts by abstracting an electron from an electron transporter and forming a radical, which then inhibits the respective electron transporter through a covalent binding step in membrane (Bedard and Krause, 2007).

In the DMSO treatment group, the 6-3 cells showed typical resting morphology with small cell bodies (Fig. 5A). On the other hand, PMA-

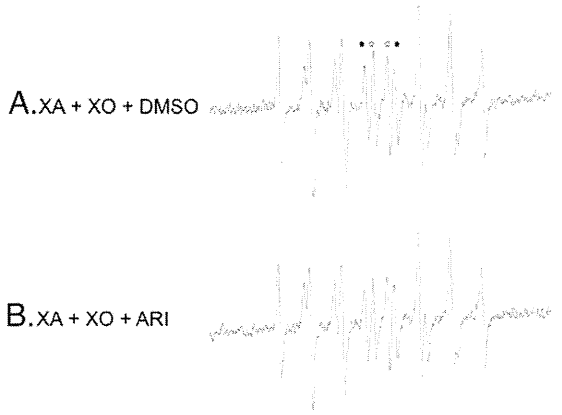


**Fig. 3.** Detection of $\cdot O_2^-$ generation in xanthine/xanthine oxidase system using ESR spin trap technique with DEPMPO. The system contained 0.4 mM xanthine, 2 mM DTPA, and 20 mM DEPMPO in PB in the presence and absence of 10 μM aripiprazole. Xanthine oxidase (0.1 U/mL) was added last to the mixture to start the reaction. (A) ESR spectra of DEPMPO adducts obtained in the xanthine/xanthine oxidase system in the presence of the control DMSO (final concentration: 0.05%). Open and closed circles represent measured signal peaks of DEPMPO–OH and DEPMPO–OOH adducts, respectively. (B) The same as (A), but also in the presence of aripiprazole (10 μM).

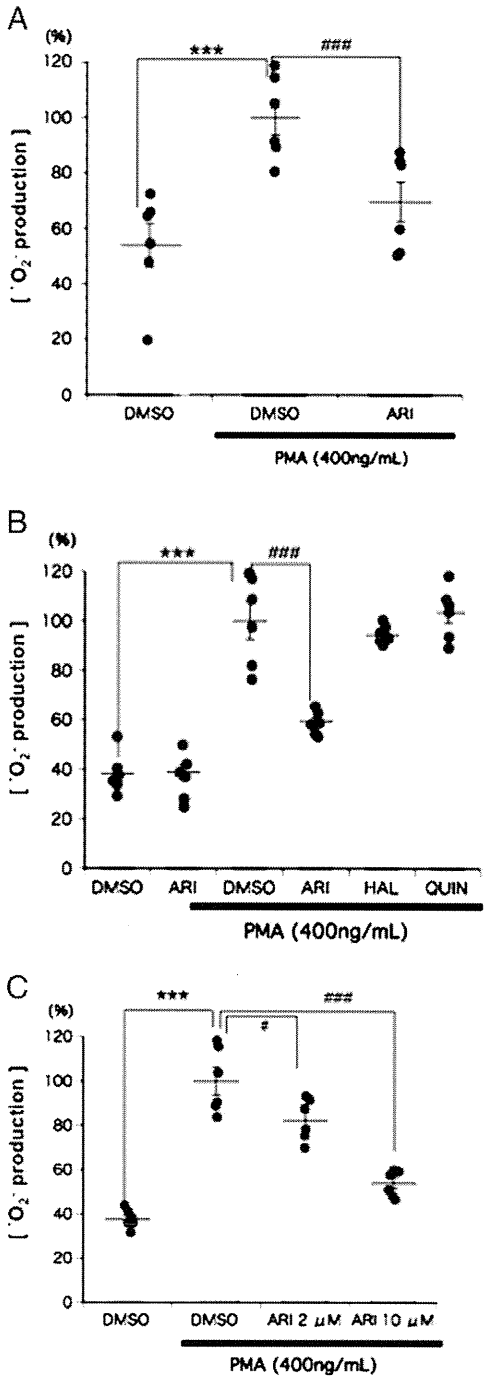


**Fig. 4.** Quantification of $\cdot O_2^-$ production in microglial cells by Nitro blue tetrazolium (NBT) assay. (A) The rat primary microglial cells were pre-treated with DMSO (0.05%) and aripiprazole (10 μM) for 5 h, then the cells were treated with PMA (400 ng/mL) for 30 min. The $\cdot O_2^-$ production was determined using the NBT assay. The results were expressed as percentage values taking the PMA + DMSO treatment group as 100%. (B) The mouse 6-3 microglial cells were pre-treated with DMSO (0.05%), aripiprazole (10 μM), haloperidol (10 μM) and quinpirole (10 μM) for 5 h, then the cells were treated with PMA (400 ng/mL) for 30 min. The $\cdot O_2^-$ production was determined using the NBT assay. The results were expressed as percentage values taking the PMA + DMSO treatment group as 100%. All data are represented as the means (SEM) of three independent experiments (n = 6–9). ***P<0.001 in comparison to the control DMSO treatment group. ###P<0.001 in comparison to the PMA + DMSO treatment group. (C) The mouse 6-3 microglial cells were pre-treated with DMSO (0.05%) and aripiprazole (10 μM) for 2 h, then the cells were treated with PMA (400 ng/mL) for 30 min. The $\cdot O_2^-$ production was determined using the NBT assay. The results were expressed as percentage values taking the PMA + DMSO treatment group as 100%. All data are represented as the means (SEM) of three independent experiments (n = 6–9). ***P<0.001 in comparison to the control DMSO treatment group. #P<0.05/###P<0.001 in comparison to the PMA + DMSO treatment group.

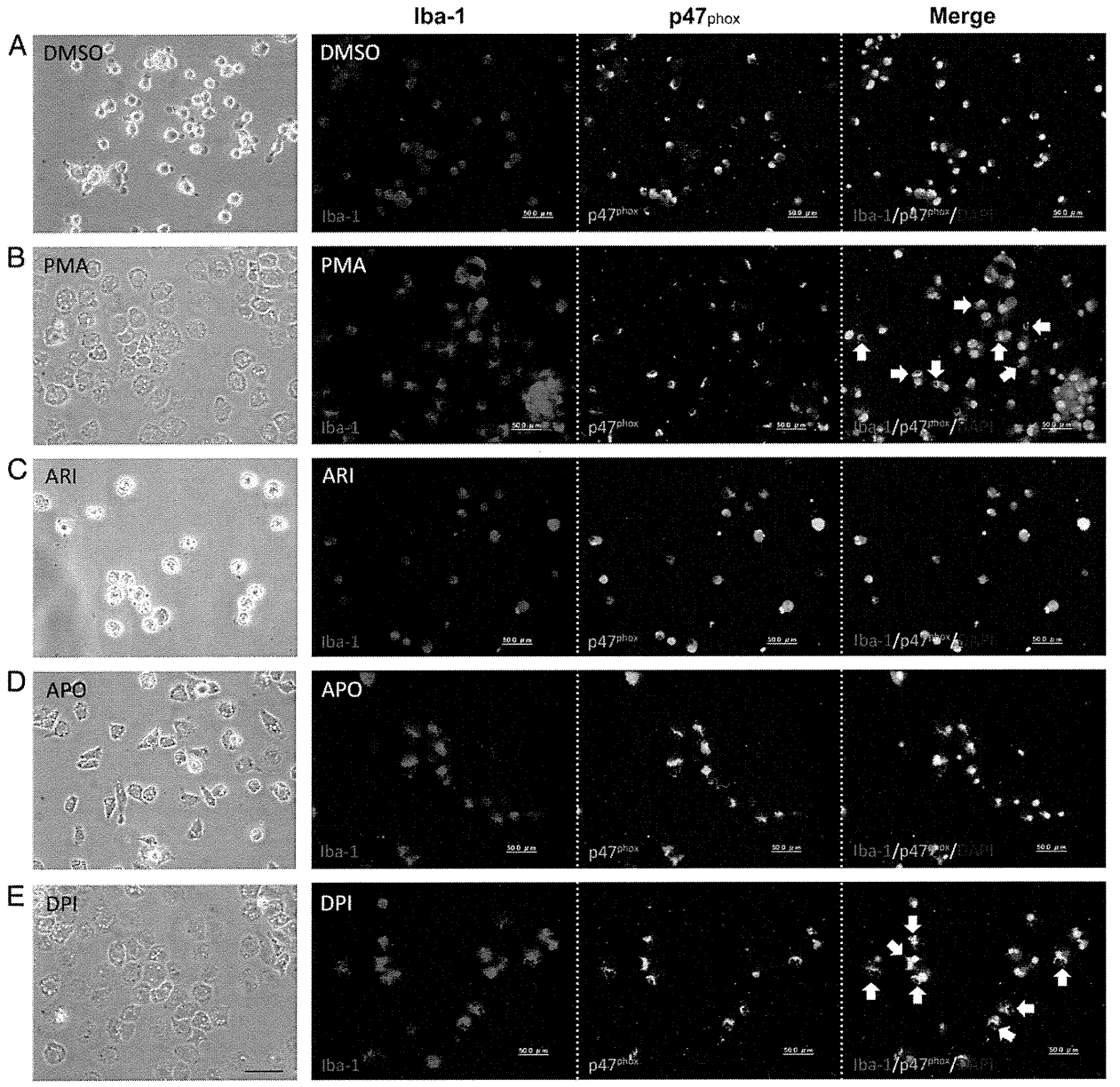


**Fig. 5.** Microglial cell morphology and cytosolic p47$^{phox}$ protein translocation. Cell morphology of the murine 6-3 microglia is shown in the leftmost line, and the existence of cytosolic Iba-1 (red), p47$^{phox}$ (green) and nuclear (DAPI; blue) is shown in the second-leftmost line, second-rightmost line and rightmost line, respectively. In the absence of PMA, cells showed resting shapes and p47$^{phox}$ was localized in the cytosol (A). Both PMA-treatment cells and DPI-pretreatment cells showed ameboid shapes and p47$^{phox}$ was translocated to the plasma/phagosomal membranes, especially phagosomal membranes inside the cytosol with a ring structure (arrows) (B and E). Both aripiprazole- and apocynin-pretreatment cells showed spindle shapes and p47$^{phox}$ was localized in the cytosol without ring structures (C and D). Scale bar indicates 50 μm.

treated 6-3 cells underwent ameboid shapes with cytoplasmic vacuoles (Fig. 5B). DPI-pretreated cells were also changed to ameboid shape morphology after PMA-stimulation (Fig. 5D). Aripiprazole- or apocynin-pretreated cells followed by PMA-stimulation were exhibited in various types of morphology, including roundish and multipolar spindle shapes (Fig. 5C and E).

Activation of NADPH oxidase has been reported to require phosphorylation and subsequent translocation of the cytosolic component p47$^{phox}$, together with other NADPH oxidase cytoplasmic subunits to the plasma membrane and/or the phagosomal membranes in the cytoplasm (Bedard and Krause, 2007; Liva et al., 1999). As aripiprazole considerably inhibits $\bullet O_2^-$ production induced by PMA, we sought to determine whether aripiprazole inhibits NADPH oxidase activation by preventing the translocation of p47$^{phox}$ from the cytosol to the membranes after PMA stimulation. Immunostaining for the p47$^{phox}$ demonstrated that cytosolic p47$^{phox}$ was formed ring-like structure after PMA treatment in the cytoplasm (Fig. 5B), suggesting that phosphorylated p47$^{phox}$ was mainly translocated to the phagosomal membranes. Aripiprazole- or apocynin-preincubated cells were prevented this formation (Fig. 5C and D). In DPI-pretreated cells, p47$^{phox}$ was also formed ring-like structure as well as PMA-treated cells (Fig. 5E). In cells treated with DMSO alone in the absence of PMA stimulation, p47$^{phox}$ remained localized primarily in the cytosol (Fig. 5A).

Therefore, one mechanism by which aripiprazole inhibits $\bullet O_2^-$ production in microglial cells seems to be through the inhibition of p47$^{phox}$ translocation to the membranes after PMA stimulation, which is similar to the inhibitory process of apocynin.

### 3.3. Aripiprazole attenuates the mobilization of intracellular $Ca^{2+}$ induced by PMA in microglia

Next, we investigated the effect of aripiprazole on the mobilization of intracellular $Ca^{2+}$ induced by PMA in rat primary microglia. PMA are known to induce $\bullet O_2^-$ from microglia with the elevation of intracellular $Ca^{2+}$ (Colton et al., 1992; Yoo et al., 1996). In the present study, we observed that PMA (400 ng/mL) acutely induced a transient increase in $[Ca^{2+}]i$ in the rat primary microglia (n = 50 cells; Fig. 6A and C), as previously reported in human microglia (Yoo et al., 1996). Pretreatment of 5 μM aripiprazole for 5 h attenuated the PMA-induced increase in $[Ca^{2+}]i$ (n = 18 cells; Fig. 6B and C). Pretreatment of 1 μM apocynin also attenuated the PMA-induced increase in $[Ca^{2+}]i$ (n = 5 cells; Fig. 6C), while pretreatment of 10 μM DPI did not affect the PMA-induced increase in $[Ca^{2+}]i$ in the rat microglial cells (n = 29 cells; Fig. 6C).

### 3.4. Aripiprazole attenuates the production of neuritic beading induced by activated microglia

Finally, neuronal damage induced by microglial activation was investigated with the co-culture experiment. Presence of neuritic bead is one of the earliest outcomes of neuronal damage (Park et al., 1996; Takeuchi et al., 2005). PMA-treatment with 6-3 microglial cells for 2 h obviously induced neuritic beading of PC12 cells (Fig. 7A, B and D). Pretreatment of aripiprazole for 5 h significantly reduced the formation of neuritic beading (Fig. 7C and D). Our results indicate that aripiprazole protected from formation of neuritic beading induced by PMA-stimulated microglial activation.

## 4. Discussion

This is the first report to demonstrate that among typical and atypical antipsychotics, only aripiprazole inhibited the generation of $\bullet O_2^-$ from PMA-stimulated microglia. Aripiprazole proved to inhibit the generation of $\bullet O_2^-$ through the cascade of PKC activation, intracellular $Ca^{2+}$ regulation and NADPH oxidase activation in microglial cells. In addition, aripiprazole indicated to have neuroprotective effects via inhibiting microglial activation by the co-culture experiment.

The typical dose range of aripiprazole is 10–30 mg/day and the typical serum concentration or plasma range of aripiprazole is 0–1000 ng/mL (0–2 μM) (Alexopoulos et al., 2004; Chew et al., 2006; Grunder et al., 2008). Antipsychotics are known to accumulate in brain tissue to levels that are 25–30 fold higher than serum levels (Baumann et al., 2004). Therefore, in spite of no evidence that the effect of a drug in cell culture could be compared to the effect of the same drug at a brain tissue level even in the same range of concentration, the concentrations of aripiprazole used in the present study might thus not be substantially different from the brain tissue levels for aripiprazole. The same concentrations were applied to other antipsychotics (haloperidol, olanzapine, clozapine and risperidone) according to previously published in vitro studies using microglial cells (Hou et al., 2006; Kato et al., 2007, 2008).

Aripiprazole is a high-affinity D2R partial agonist, while other antipsychotics investigated in the present study are all D2R antagonists (Burris et al., 2002; Shapiro et al., 2003). These differences may be relevant to the results shown in the present study. Farber et al. provided the first evidence of the existence of functional dopamine receptors on microglia. In their study, quinpirole inhibited the release of NO from LPS-induced microglia dose-dependently (Farber et al., 2005). On the other hand, in our previous study, not quinpirole but aripiprazole showed inhibitory effects on the generation of NO and TNF-α from interferon-γ-stimulated microglia (Kato et al., 2008). Moreover, in the present study, quinpirole did not have any inhibitory effects on the generation of $\bullet O_2^-$ from PMA-stimulated microglia. These results seem to suggest that the dopamine $D_2$ receptors may not be involved in the generation of $\bullet O_2^-$ from PMA-stimulated microglia and in the inhibition of $\bullet O_2^-$ production by aripiprazole shown in the present study. Aripiprazole has affinities of other receptors such as

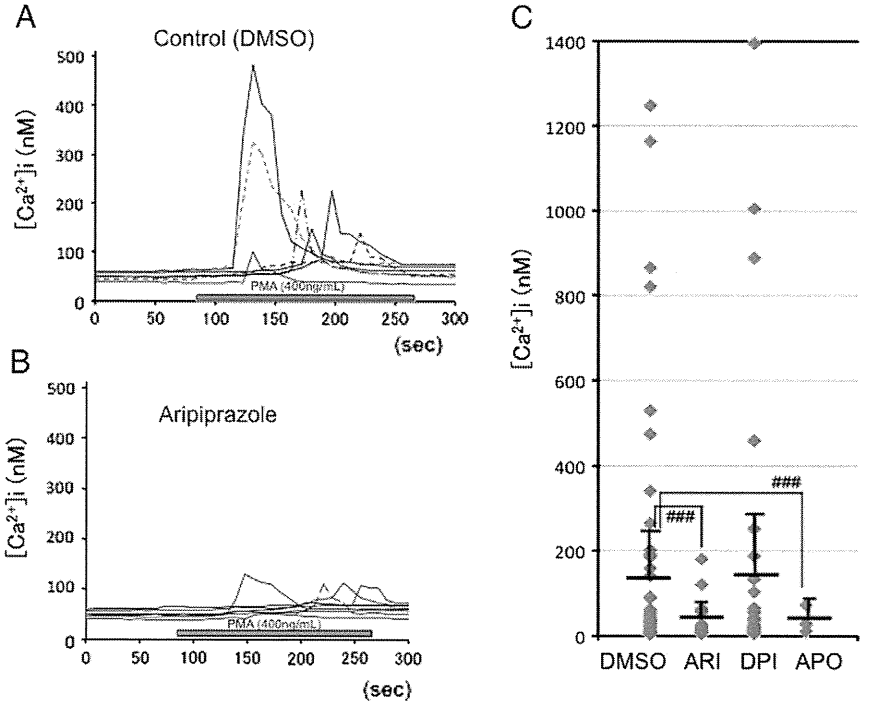


**Fig. 6.** Aripiprazole attenuates the mobilization of intracellular $Ca^{2+}$ induced by PMA in rat microglia. (A and B) Seven representative traces showing a brief application (3 min) of 400 ng/mL PMA induced a transient increase in $[Ca^{2+}]i$ in rat microglia pretreated with DMSO (0.025%; in A) and with aripiprazole (5 μM; in B). (C) Bar graph summarizing the effect of different manipulations on the peak amplitude of PMA-induced increase in $[Ca^{2+}]i$ in rat microglia. Increase of $[Ca^{2+}]i$ in response to PMA application with DMSO, aripiprazole, DPI and apocynin was calculated as a difference between basal $[Ca^{2+}]i$ and highest $[Ca^{2+}]i$ during the treatment of PMA, respectively. All data presented were obtained from at least five dishes and three different cell preparations. Data are expressed as the mean ± SEM. ###P<0.001 in comparison to the PMA + DMSO treatment group.

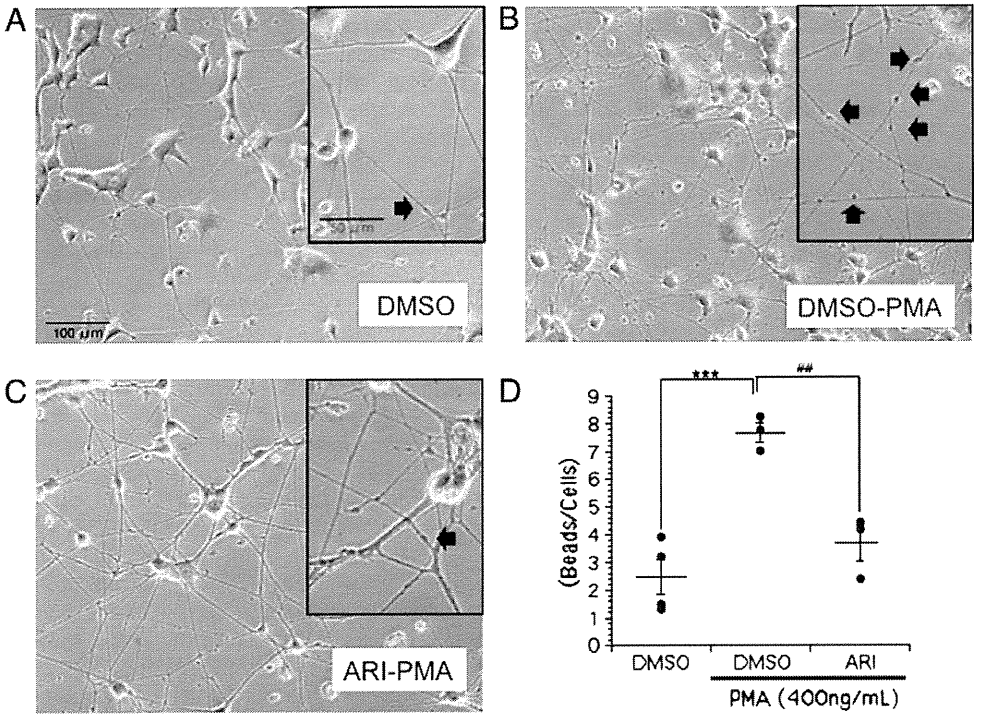


**Fig. 7.** Neuritic beading induced by PMA-stimulated microglia. Neuritic formation of the PC12 cells, which was taken under a phase-contrast microscope, is shown in the main photo and enhanced photo is shown in the upper right-hand corner (enhanced) (A–C). (A) Pretreatment with DMSO (0.05%), following co-culture with the 6-3 microglial cells without PMA treatment for 2 h. (B) Pretreatment with DMSO (0.05%), following co-culture with the 6-3 microglial cells with 400 ng/mL PMA treatment for 2 h. (C) Pretreatment with aripiprazole (10 μM), following co-culture with the 6-3 microglial cells with 400 ng/mL PMA treatment for 2 h. (D) Quantification of neuritic beading. The number of neuritic beading (beads) under more than 100 neuronal cell bodies was assessed blindly in three independent trials. All data are expressed the means (SEM) of the number of neuritic beading (beads) per one neuronal cell (each: 3–4 trials). ***P<0.001 in comparison to the control DMSO treatment group. ##P<0.01 in comparison to the DMSO + PMA treatment group.

serotonin (Shapiro et al., 2003). Our recent study has proved that not only antipsychotics but also antidepressants have inhibitory effects of microglial activation (Horikawa et al., 2010), which indicate that other pharmacological mechanism beyond D2R may exist in our findings. Further investigation is required in order to clarify the underlying mechanism.

We showed the first evidence that aripiprazole attenuates the mobilization of intracellular $Ca^{2+}$ induced by PMA in rat microglia. PMA is known to induce $\cdot O_2^-$ from microglia with the elevation of intracellular $Ca^{2+}$ (Colton et al., 1992; Yoo et al., 1996). Intracellular $Ca^{2+}$ is one of the endogenous activators of PKC. Regarding mammalian astrocytes, PMA proved to activate the NADPH oxidase through the activation of PKC, while the elevation of intracellular $Ca^{2+}$ induced by PMA itself activates the NADPH oxidase independently of PKC (Abramov et al., 2005). We showed that aripiprazole inhibits NADPH oxidase activation by preventing the translocation of $p47^{phox}$ from the cytosol to the membrane after PMA stimulation. Our results suggest that the $\cdot O_2^-$ generation in the microglial cells depends on NADPH oxidase pathway, inhibitory effects of which are similar not to DPI but to apocynin. Summing up these results, aripiprazole indicates to inhibit the $\cdot O_2^-$ generation through the NADPH oxidase by suppressing the elevation of intracellular $Ca^{2+}$ in PMA-treated microglia.

Antioxidants have recently been regarded to have protective effects in neurodegeneration, and microglial activation via NADPH oxidase has a key role in this process (Wang et al., 2006). NADPH-derived ROS such as $\cdot O_2^-$ and $\cdot OH$ radicals have been reported not only to cause microglial proliferation but also to amplify the proinflammatory gene expressions, both of which are associated with neurotoxicity induced by activated microglia (Pawate et al., 2004; Qin et al., 2004). In our previous study, risperidone and other atypical antipsychotics with D2R antagonism inhibited the production of proinflammatory cytokines (Bian et al., 2008; Kato et al., 2007), however these antipsychotics have no inhibitory effect of releasing $\cdot O_2^-$ radicals from activated microglia in the present study. On the other hand, aripiprazole proved to have dual inhibitory effects of releasing pro-inflammatory cytokines (Kato et al., 2008) and $\cdot O_2^-$ radicals from activated microglia in the present study. Therefore, we presume aripiprazole to be the strongest antioxidative/anti-inflammatory agent among antipsychotics.

We previously demonstrated that aripiprazole inhibits microglial activation induced by IFN-γ and suggested that this inhibitory effect is related to the inhibition of the cell signaling pathways including PKC, p38MAPK, and ERK (Kato et al., 2008). PMA is a PKC activator and PKC pathway is located in the upstream of both p38MAPK and ERK pathways in the process of PMA-induced microglial activation as shown in Nikodemova et al. (2006). Therefore, the inhibitory effects of aripiprazole on neuritic beading which was shown in the present co-culture study is probably due to the inhibitory effects of aripiprazole on the generation of both $\cdot O_2^-$ and pro-inflammatory cytokines from PMA-stimulated microglia.

Structural brain abnormalities such as progressive gray matter loss have been extensively and consistently described in schizophrenic patients (Davis et al., 2003; Kumra et al., 2005). This evidence is the primarily propounded mechanism explaining the neurodegenerative course of schizophrenia (Salisbury et al., 2007). Multiple lines of evidence combine to implicate the increased susceptibility to apoptotic death in the pathophysiology of schizophrenia (Glantz et al., 2006). The activation of apoptotic process can lead to a rapid neuronal death (Glantz et al., 2006; Jarskog et al., 2005). Microglial NADPH oxidase pathway has recently been reported to play a key role in the process of neuronal deaths (Qin et al., 2006). Furthermore, our results of co-culture experiment suggest that activation of microglial NADPH oxidase pathway induces neuritic beading formation, which is one of the initial steps of neuronal damage (Park et al., 1996; Takeuchi et al., 2005). In addition, aripiprazole attenuated the neuritic beading formation, which indicates that aripiprazole may be a neuroprotective agent via inhibiting microglial activation. One recent animal study

indicates that aripiprazole prevents apoptosis in the brain of methamphetamine-treatment rodents. (Abekawa et al., 2011), which supports the significance of our results.

Recent neuroimaging studies have shown significant volume reductions in white matter with abnormal brain connectivity in schizophrenia (Schlosser et al., 2007). The reduced density and compromised morphology of the oligodendrocytes as well as signs of deviant myelination have been evident in schizophrenia (Uranova et al., 2007). Microglial activation in the CNS has been implicated in the pathogenesis of white matter disorders, and microglial cytotoxicity of oligodendrocyte has been reported to mediate through the free radical-related molecules such as NO, $\bullet O_2^-$ and their compound, peroxynitrite ($ONOO^-$) generated by activated microglia (Li et al., 2005; Merrill et al., 1993). On the other hand, one recent imaging report suggests that risperidone, which have anti-inflammatory effects on microglial activation in vitro (Kato et al., 2007), may be specifically impacting later-myelinating intracortical circuitry in patients with schizophrenia (Bartzokis et al., 2009).

Summing up the aforementioned evidence and our results, aripiprazole may thus have therapeutic effects on patients with schizophrenia by reducing the microglial inflammatory/oxidative reactions, which puts forward a novel therapeutic hypothesis beyond dopamine/neuron doctrine in the field of schizophrenia research. Besides schizophrenia, aripiprazole has proved to have therapeutic effects in depression, anxiety and other psychiatric disorders (Mohamed et al., 2009; Weber et al., 2008). In a recent animal study, aripiprazole has proved to have protective effects on the depression-induced oxidative stress in rat brain (Eren et al., 2007). This evidence has accorded with our present result that except for aripiprazole no other antipsychotics have an antioxidative effect via inhibiting superoxide generation from activated microglia. Thus, such wider range of aripiprazole pharmacological effects on various psychiatric diseases may be explained by the present result that aripiprazole inhibits the microglia-induced oxidative stress.

The brain is considered particularly vulnerable to oxidative damage. This intrinsic oxidative vulnerability of the brain suggests that oxidative damage may be a plausible pathogenic candidate of schizophrenia, depression and other psychiatric disorders (Ng et al., 2008). Therefore, our results may imply that aripiprazole acts, at least partially, by a different mechanism of action than other antipsychotics, which may be reflected in its deviating clinical profile. Regarding further studies, the molecular mechanism of the inhibitory effect of aripiprazole on the generation of $\bullet O_2^-$ radicals from PMA-stimulated microglia should be clarified in more detail, and in vivo studies should also be performed in order to confirm the present results.

**Role of funding source**

This work was financially supported by Grant-in-Aid for Research Fellow of the Japan Society for the Promotion of Science (JSPS) [to TAK] and for researchers from JSPS [to TAK, AM, YM and SK], and by Grant-in-Aid for Mitsubishi Pharma Research Foundation [to TAK and AM].

**Contributors**

All authors contributed substantially to the scientific process leading up to the writing of the present paper. TAK, the first author, and AM, the principal investigator of the present research made the conception and design of the project and wrote the protocol. The performance of experiments and the data analysis/interpretation were done by TAK, AM, KY, YM, HH, YS, SH, YHH, NS, EH and YM. TAK wrote the first draft of the manuscript. Critical revisions of the manuscript were made by TI, HU and SK. All authors contributed to and have approved the final manuscript.

**Conflict of interest**

All authors declare that they have no financial conflict of interest.

**Acknowledgments**

The authors thank Prof. Makoto Sawada of Nagoya University for providing the microglial cell line, 6-3. The authors also thank Dr. Tomoaki Inoue and Ms. Mayumi Tanaka for his/her experimental assistance.

## References

Abekawa, T., Ito, K., Nakagawa, S., Nakato, Y., Koyama, T., 2011. Effects of aripiprazole and haloperidol on progression to schizophrenia-like behavioural abnormalities and apoptosis in rodents. Schizophr. Res. 125, 77–87.

Abramov, A.Y., Jacobson, J., Wientjes, F., Hothersall, J., Canevari, L., Duchen, M.R., 2005. Expression and modulation of an NADPH oxidase in mammalian astrocytes. J. Neurosci. 25, 9176–9184.

Akhondzadeh, S., Tabatabaee, M., Amini, H., Ahmadi Abhari, S.A., Abbasi, S.H., Behnam, B., 2007. Celecoxib as adjunctive therapy in schizophrenia: a double-blind, randomized and placebo-controlled trial. Schizophr. Res. 90, 179–185.

Alexopoulos, G.S., Streim, J., Carpenter, D., Docherty, J.P., 2004. Using antipsychotic agents in older patients. J. Clin. Psychiatry 65 (Suppl 2), 5–104.

Bartzokis, G., Lu, P.H., Stewart, S.B., Oluwadara, B., Lucas, A.J., Pantages, J., Pratt, E., Sherin, J.E., Altshuler, L.L., Mintz, J., Gitlin, M.J., Subotnik, K.L., Nuechterlein, K.H., 2009. In vivo evidence of differential impact of typical and atypical antipsychotics on intracortical myelin in adults with schizophrenia. Schizophr. Res. 113, 322–331.

Baumann, P., Hiemke, C., Ulrich, S., Eckermann, G., Gaertner, I., Gerlach, M., Kuss, H.J., Laux, G., Muller-Oerlinghausen, B., Rao, M.L., Riederer, P., Zernig, G., Arbeitsgemeinschaft fur neuropsychopharmakologie und p, 2004. The AGNP-TDM expert group consensus guidelines: therapeutic drug monitoring in psychiatry. Pharmacopsychiatry 37, 243–265.

Bedard, K., Krause, K.H., 2007. The NOX family of ROS-generating NADPH oxidases: physiology and pathophysiology. Physiol. Rev. 87, 245–313.

Behrens, M.M., Ali, S.S., Dao, D.N., Lucero, J., Shekhtman, G., Quick, K.L., Dugan, L.L., 2007. Ketamine-induced loss of phenotype of fast-spiking interneurons is mediated by NADPH-oxidase. Science 318, 1645–1647.

Berk, M., Copolov, D., Dean, O., Lu, K., Jeavons, S., Schapkaitz, I., Anderson-Hunt, M., Judd, F., Katz, F., Katz, P., Ording-Jespersen, S., Little, J., Conus, P., Cuenod, M., Do, K.Q., Bush, A.I., 2008. N-acetyl cysteine as a glutathione precursor for schizophrenia—a double-blind, randomized, placebo-controlled trial. Biol. Psychiatry 64, 361–368.

Bian, Q., Kato, T., Monji, A., Hashioka, S., Mizoguchi, Y., Horikawa, H., Kanba, S., 2008. The effect of atypical antipsychotics, perospirone, ziprasidone and quetiapine on microglial activation induced by interferon-gamma. Prog. Neuropsychopharmacol. Biol. Psychiatry 32, 42–48.

Block, M.L., Hong, J.S., 2005. Microglia and inflammation-mediated neurodegeneration: multiple triggers with a common mechanism. Prog. Neurobiol. 76, 77–98.

Block, M.L., Zecca, L., Hong, J.S., 2007. Microglia-mediated neurotoxicity: uncovering the molecular mechanisms. Nat. Rev. Neurosci. 8, 57–69.

Burris, K.D., Molski, T.F., Xu, C., Ryan, E., Tottori, K., Kikuchi, T., Yocca, F.D., Molinoff, P.B., 2002. Aripiprazole, a novel antipsychotic, is a high-affinity partial agonist at human dopamine D2 receptors. J. Pharmacol. Exp. Ther. 302, 381–389.

Chen, G., Henter, I.D., Manji, H.K., 2009. A role for PKC in mediating stress-induced prefrontal cortical structural plasticity and cognitive function. Proc. Natl Acad. Sci. U.S.A. 106, 17613–17614.

Chew, M.L., Mulsant, B.H., Pollock, B.G., Lehman, M.E., Greenspan, A., Kirshner, M.A., Bies, R.R., Kapur, S., Gharabawi, G., 2006. A model of anticholinergic activity of atypical antipsychotic medications. Schizophr. Res. 88, 63–72.

Choi, H.S., Kim, J.W., Cha, Y.N., Kim, C., 2006. A quantitative nitroblue tetrazolium assay for determining intracellular superoxide anion production in phagocytic cells. J. Immunoassay Immunochem. 27, 31–44.

Colton, C.A., Yao, J., Keri, J.E., Gilbert, D., 1992. Regulation of microglial function by interferons. J. Neuroimmunol. 40, 89–98.

Dalman, C., Allebeck, P., Gunnell, D., Harrison, G., Kristensson, K., Lewis, G., Lofving, S., Rasmussen, F., Wicks, S., Karlsson, H., 2008. Infections in the CNS during childhood and the risk of subsequent psychotic illness: a cohort study of more than one million Swedish subjects. Am. J. Psychiatry 165, 59–65.

Davis, K.L., Stewart, D.G., Friedman, J.I., Buchsbaum, M., Harvey, P.D., Hof, P.R., Buxbaum, J., Haroutunian, V., 2003. White matter changes in schizophrenia: evidence for myelin-related dysfunction. Arch. Gen. Psychiatry 60, 443–456.

Do, K.Q., Cabungcal, J.H., Frank, A., Steullet, P., Cuenod, M., 2009. Redox dysregulation, neurodevelopment, and schizophrenia. Curr. Opin. Neurobiol. 19, 220–230.

Doorduin, J., de Vries, E., Willemsen, A., de Groot, J., Dierckx, R., Klein, H., 2009. Neuroinflammation in schizophrenia-related psychosis: a PET study. J. Nucl. Med. 50, 1801–1807.

Eren, I., Naziroglu, M., Demirdas, A., 2007. Protective effects of lamotrigine, aripiprazole and escitalopram on depression-induced oxidative stress in rat brain. Neurochem. Res. 32, 1188–1195.

Farber, K., Pannasch, U., Kettenmann, H., 2005. Dopamine and noradrenaline control distinct functions in rodent microglial cells. Mol. Cell. Neurosci. 29, 128–138.

Glantz, L.A., Gilmore, J.H., Lieberman, J.A., Jarskog, L.F., 2006. Apoptotic mechanisms and the synaptic pathology of schizophrenia. Schizophr. Res. 81, 47–63.

Grunder, G., Fellows, C., Janouschek, H., Veselinovic, T., Boy, C., Brocheler, A., Kirschbaum, K.M., Hellmann, S., Spreckelmeyer, K.M., Hiemke, C., Rosch, F., Schaefer, W.M., Vernaleken, I., 2008. Brain and plasma pharmacokinetics of aripiprazole in patients with schizophrenia: an [18F]fallypride PET study. Am. J. Psychiatry 165, 988–995.

Grynkiewicz, G., Poenie, M., Tsien, R.Y., 1985. A new generation of $Ca^{2+}$ indicators with greatly improved fluorescence properties. J. Biol. Chem. 260, 3440–3450.

Hains, A.B., Vu, M.A., Maciejewski, P.K., van Dyck, C.H., Gottron, M., Arnsten, A.F., 2009. Inhibition of protein kinase C signaling protects prefrontal cortex dendritic spines and cognition from the effects of chronic stress. Proc. Natl Acad. Sci. U.S.A. 106, 17957–17962.

Hanisch, U.K., Kettenmann, H., 2007. Microglia: active sensor and versatile effector cells in the normal and pathologic brain. Nat. Neurosci. 10, 1387–1394.

Hashioka, S., Han, Y.H., Fujii, S., Kato, T., Monji, A., Utsumi, H., Sawada, M., Nakanishi, H., Kanba, S., 2007a. Phosphatidylserine and phosphatidylcholine-containing liposomes inhibit amyloid beta and interferon-gamma-induced microglial activation. Free Radic. Biol. Med. 42, 945–954.
Hashioka, S., Han, Y.H., Fujii, S., Kato, T., Monji, A., Utsumi, H., Sawada, M., Nakanishi, H., Kanba, S., 2007b. Phospholipids modulate superoxide and nitric oxide production by lipopolysaccharide and phorbol 12-myristate-13-acetate-activated microglia. Neurochem. Int. 50, 499–506.
Horikawa, H., Kato, T.A., Mizoguchi, Y., Monji, A., Seki, Y., Ohkuri, T., Gotoh, L., Yonaha, M., Ueda, T., Hashioka, S., Kanba, S., 2010. Inhibitory effects of SSRIs on IFN-gamma induced microglial activation through the regulation of intracellular calcium. Prog. Neuropsychopharmacol. Biol. Psychiatry 34, 1306–1316.
Hou, Y., Wu, C.F., Yang, J.Y., He, X., Bi, X.L., Yu, L., Guo, T., 2006. Effects of clozapine, olanzapine and haloperidol on nitric oxide production by lipopolysaccharide-activated N9 cells. Prog. Neuropsychopharmacol. Biol. Psychiatry 30 (8), 1523–1528.
Jarskog, L.F., Glantz, L.A., Gilmore, J.H., Lieberman, J.A., 2005. Apoptotic mechanisms in the pathophysiology of schizophrenia. Prog. Neuropsychopharmacol. Biol. Psychiatry 29, 846–858.
Jia, P., Wang, L., Meltzer, H.Y., Zhao, Z., 2010. Common variants conferring risk of schizophrenia: a pathway analysis of GWAS data. Schizophr. Res. 122, 38–42.
Kanzawa, T., Sawada, M., Kato, K., Yamamoto, K., Mori, H., Tanaka, R., 2000. Differentiated regulation of allo-antigen presentation by different types of murine microglial cell lines. J. Neurosci. Res. 62, 383–388.
Kapur, S., Mamo, D., 2003. Half a century of antipsychotics and still a central role for dopamine D2 receptors. Prog. Neuropsychopharmacol. Biol. Psychiatry 27, 1081–1090.
Kato, T., Monji, A., Hashioka, S., Kanba, S., 2007. Risperidone significantly inhibits interferon-gamma-induced microglial activation in vitro. Schizophr. Res. 92, 108–115.
Kato, T., Mizoguchi, Y., Monji, A., Horikawa, H., Suzuki, S.O., Seki, Y., Iwaki, T., Hashioka, S., Kanba, S., 2008. Inhibitory effects of aripiprazole on interferon-gamma-induced microglial activation via intracellular $Ca^{2+}$ regulation in vitro. J. Neurochem. 106, 815–825.
Kumra, S., Ashtari, M., Cervellione, K.L., Henderson, I., Kester, H., Roofeh, D., Wu, J., Clarke, T., Thaden, E., Kane, J.M., Rhinewine, J., Lencz, T., Diamond, A., Ardekani, B.A., Szeszko, P.R., 2005. White matter abnormalities in early-onset schizophrenia: a voxel-based diffusion tensor imaging study. J. Am. Acad. Child Adolesc. Psychiatry 44, 934–941.
Lavoie, S., Murray, M.M., Deppen, P., Knyazeva, M.G., Berk, M., Boulat, O., Bovet, P., Bush, A.I., Conus, P., Copolov, D., Fornari, E., Meuli, R., Solida, A., Vianin, P., Cuenod, M., Buclin, T., Do, K.Q., 2008. Glutathione precursor, N-acetyl-cysteine, improves mismatch negativity in schizophrenia patients. Neuropsychopharmacology 33, 2187–2199.
Leucht, S., Corves, C., Arbter, D., Engel, R.R., Li, C., Davis, J.M., 2009. Second-generation versus first-generation antipsychotic drugs for schizophrenia: a meta-analysis. Lancet 373, 31–41.
Li, J., Baud, O., Vartanian, T., Volpe, J.J., Rosenberg, P.A., 2005. Peroxynitrite generated by inducible nitric oxide synthase and NADPH oxidase mediates microglial toxicity to oligodendrocytes. Proc. Natl Acad. Sci. U.S.A. 102, 9936–9941.
Liva, S.M., Kahn, M.A., Dopp, J.M., de Vellis, J., 1999. Signal transduction pathways induced by GM-CSF in microglia: significance in the control of proliferation. Glia 26, 344–352.
Merrill, J.E., Ignarro, L.J., Sherman, M.P., Melinek, J., Lane, T.E., 1993. Microglial cell cytotoxicity of oligodendrocytes is mediated through nitric oxide. J. Immunol. 151, 2132–2141.
Miyamoto, S., Duncan, G.E., Marx, C.E., Lieberman, J.A., 2005. Treatments for schizophrenia: a critical review of pharmacology and mechanisms of action of antipsychotic drugs. Mol. Psychiatry 10, 79–104.
Miyaoka, T., Yasukawa, R., Yasuda, H., Hayashida, M., Inagaki, T., Horiguchi, J., 2008. Minocycline as adjunctive therapy for schizophrenia: an open-label study. Clin. Neuropharmacol. 31, 287–292.
Mizoguchi, Y., Kanematsu, T., Hirata, M., Nabekura, J., 2003. A rapid increase in the total number of cell surface functional GABAA receptors induced by brain-derived neurotrophic factor in rat visual cortex. J. Biol. Chem. 278, 44097–44102.
Mizoguchi, Y., Monji, A., Kato, T., Seki, Y., Gotoh, L., Horikawa, H., Suzuki, S.O., Iwaki, T., Yonaha, M., Hashioka, S., Kanba, S., 2009. Brain-derived neurotrophic factor induces sustained elevation of intracellular $Ca^{2+}$ in rodent microglia. J. Immunol. 183, 7778–7786.
Mohamed, S., Leslie, D.L., Rosenheck, R.A., 2009. Use of antipsychotics in the treatment of major depressive disorder in the U.S. Department of Veterans Affairs. J. Clin. Psychiatry 70, 906–912.
Monji, A., Kato, T., Kanba, S., 2009. Cytokines and schizophrenia: microglia hypothesis of schizophrenia. Psychiatry Clin. Neurosci. 63, 257–265.
Mortensen, P.B., Pedersen, C.B., Hougaard, D.M., Norgaard-Petersen, B., Mors, O., Borglum, A.D., Yolken, R.H., 2010. A Danish National Birth Cohort study of maternal HSV-2 antibodies as a risk factor for schizophrenia in their offspring. Schizophr. Res. 122, 257–263.
Muller, N., Krause, D., Dehning, S., Musil, R., Schennach-Wolff, R., Obermeier, M., Moller, H.J., Klauss, V., Schwarz, M.J., Riedel, M., 2010. Celecoxib treatment in an early stage of schizophrenia: results of a randomized, double-blind, placebo-controlled trial of celecoxib augmentation of amisulpride treatment. Schizophr. Res. 121, 118–124.
Ng, F., Berk, M., Dean, O., Bush, A.I., 2008. Oxidative stress in psychiatric disorders: evidence base and therapeutic implications. Int. J. Neuropsychopharmacol. 11, 851–876.
Nikodemova, M., Duncan, I.D., Watters, J.J., 2006. Minocycline exerts inhibitory effects on multiple mitogen-activated protein kinases and IkappaBalpha degradation in a stimulus-specific manner in microglia. J. Neurochem. 96, 314–323.
Park, J.S., Bateman, M.C., Goldberg, M.P., 1996. Rapid alterations in dendrite morphology during sublethal hypoxia or glutamate receptor activation. Neurobiol. Dis. 3, 215–227.
Pawate, S., Shen, Q., Fan, F., Bhat, N.R., 2004. Redox regulation of glial inflammatory response to lipopolysaccharide and interferongamma. J. Neurosci. Res. 77, 540–551.
Potkin, S.G., Saha, A.R., Kujawa, M.J., Carson, W.H., Ali, M., Stock, E., Stringfellow, J., Ingenito, G., Marder, S.R., 2003. Aripiprazole, an antipsychotic with a novel mechanism of action, and risperidone vs placebo in patients with schizophrenia and schizoaffective disorder. Arch. Gen. Psychiatry 60, 681–690.
Qian, L., Wei, S.J., Zhang, D., Hu, X., Xu, Z., Wilson, B., El-Benna, J., Hong, J.S., Flood, P.M., 2008. Potent anti-inflammatory and neuroprotective effects of TGF-beta1 are mediated through the inhibition of ERK and p47phox-Ser345 phosphorylation and translocation in microglia. J. Immunol. 181, 660–668.
Qin, L., Liu, Y., Wang, T., Wei, S.J., Block, M.L., Wilson, B., Liu, B., Hong, J.S., 2004. NADPH oxidase mediates lipopolysaccharide-induced neurotoxicity and proinflammatory gene expression in activated microglia. J. Biol. Chem. 279, 1415–1421.
Qin, B., Cartier, L., Dubois-Dauphin, M., Li, B., Serrander, L., Krause, K.H., 2006. A key role for the microglial NADPH oxidase in APP-dependent killing of neurons. Neurobiol. Aging 27, 1577–1587.
Radewicz, K., Garey, L.J., Gentleman, S.M., Reynolds, R., 2000. Increase in HLA-DR immunoreactive microglia in frontal and temporal cortex of chronic schizophrenics. J. Neuropathol. Exp. Neurol. 59, 137–150.
Salisbury, D.F., Kuroki, N., Kasai, K., Shenton, M.E., McCarley, R.W., 2007. Progressive and interrelated functional and structural evidence of post-onset brain reduction in schizophrenia. Arch. Gen. Psychiatry 64, 521–529.
Sankarapandi, S., Zweier, J.L., Mukherjee, G., Quinn, M.T., Huso, D.L., 1998. Measurement and characterization of superoxide generation in microglial cells: evidence for an NADPH oxidase-dependent pathway. Arch. Biochem. Biophys. 353, 312–321.
Sawa, A., Pletnikov, M.V., Kamiya, A., 2004. Neuron–glia interactions clarify genetic–environmental links in mental illness. Trends Neurosci. 27, 294–297.
Sawada, M., Imai, F., Suzuki, H., Hayakawa, M., Kanno, T., Nagatsu, T., 1998. Brain-specific gene expression by immortalized microglial cell-mediated gene transfer in the mammalian brain. FEBS Lett. 433, 37–40.
Schiavone, S., Sorce, S., Dubois-Dauphin, M., Jaquet, V., Colaianna, M., Zotti, M., Cuomo, V., Trabace, L., Krause, K.H., 2009. Involvement of NOX2 in the development of behavioral and pathologic alterations in isolated rats. Biol. Psychiatry 66, 384–392.
Schlosser, R.G., Nenadic, I., Wagner, G., Gullmar, D., von Consbruch, K., Kohler, S., Schultz, C.C., Koch, K., Fitzek, C., Matthews, P.M., Reichenbach, J.R., Sauer, H., 2007. White matter abnormalities and brain activation in schizophrenia: a combined DTI and fMRI study. Schizophr. Res. 89, 1–11.
Seki, Y., Suzuki, S.O., Masui, K., Harada, S., Nakamura, S., Kanba, S., Iwaki, T., in press. A simple and high-yield method for preparation of rat microglial cultures utilizing Aclar plastic film. Neuropathology. doi:10.1111/j.1440-1789.2010.01163.x. [Electronic publication ahead of print].
Seshadri, S., Kamiya, A., Yokota, Y., Prikulis, I., Kano, S., Hayashi-Takagi, A., Stanco, A., Eom, T.Y., Rao, S., Ishizuka, K., Wong, P., Korth, C., Anton, E.S., Sawa, A., 2010. Disrupted-in-Schizophrenia-1 expression is regulated by beta-site amyloid precursor protein cleaving enzyme-1-neuregulin cascade. Proc. Natl Acad. Sci. U.S.A. 107, 5622–5627.
Shapiro, D.A., Renock, S., Arrington, E., Chiodo, L.A., Liu, L.X., Sibley, D.R., Roth, B.L., Mailman, R., 2003. Aripiprazole, a novel atypical antipsychotic drug with a unique and robust pharmacology. Neuropsychopharmacology 28, 1400–1411.
Sirota, P., Gavrieli, R., Wolach, B., 2003. Overproduction of neutrophil radical oxygen species correlates with negative symptoms in schizophrenic patients: parallel studies on neutrophil chemotaxis, superoxide production and bactericidal activity. Psychiatry Res. 121, 123–132.
Steiner, J., Bielau, H., Brisch, R., Danos, P., Ullrich, O., Mawrin, C., Bernstein, H.G., Bogerts, B., 2008. Immunological aspects in the neurobiology of suicide: elevated microglial density in schizophrenia and depression is associated with suicide. J. Psychiatr. Res. 42, 151–157.
Takano, A., Arakawa, R., Ito, H., Tateno, A., Takahashi, H., Matsumoto, R., Okubo, Y., Suhara, T., 2010. Peripheral benzodiazepine receptors in patients with chronic schizophrenia: a PET study with [11C]DAA1106. Int. J. Neuropsychopharmacol. 13, 943–950.
Takeuchi, H., Mizuno, T., Zhang, G., Wang, J., Kawanokuchi, J., Kuno, R., Suzumura, A., 2005. Neuritic beading induced by activated microglia is an early feature of neuronal dysfunction toward neuronal death by inhibition of mitochondrial respiration and axonal transport. J. Biol. Chem. 280, 10444–10454.
Tan, A.S., Berridge, M.V., 2000. Superoxide produced by activated neutrophils efficiently reduces the tetrazolium salt, WST-1 to produce a soluble formazan: a simple colorimetric assay for measuring respiratory burst activation and for screening anti-inflammatory agents. J. Immunol. Methods 238, 59–68.
Treasaden, I.H., Puri, B.K., 2008. Cerebral spectroscopic and oxidative stress studies in patients with schizophrenia who have dangerously violently offended. BMC Psychiatry 8 (Suppl 1), S7.
Uranova, N.A., Vostrikov, V.M., Vikhreva, O.V., Zimina, I.S., Kolomeets, N.S., Orlovskaya, D.D., 2007. The role of oligodendrocyte pathology in schizophrenia. Int. J. Neuropsychopharmacol. 10, 537–545.
van Berckel, B.N., Bossong, M.G., Boellaard, R., Kloet, R., Schuitemaker, A., Caspers, E., Luurtsema, G., Windhorst, A.D., Cahn, W., Lammertsma, A.A., Kahn, R.S., 2008. Microglia activation in recent-onset schizophrenia: a quantitative (R)-[11C] PK11195 positron emission tomography study. Biol. Psychiatry 64, 820–822.
van Winkel, R., Stefanis, N.C., Myin-Germeys, I., 2008. Psychosocial stress and psychosis. A review of the neurobiological mechanisms and the evidence for gene–stress interaction. Schizophr. Bull. 34, 1095–1105.

Wang, J.Y., Wen, L.L., Huang, Y.N., Chen, Y.T., Ku, M.C., 2006. Dual effects of antioxidants in neurodegeneration: direct neuroprotection against oxidative stress and indirect protection via suppression of glia-mediated inflammation. Curr. Pharm. Des. 12, 3521–3533.

Wang, J.F., Shao, L., Sun, X., Young, L.T., 2009. Increased oxidative stress in the anterior cingulate cortex of subjects with bipolar disorder and schizophrenia. Bipolar Disord. 11, 523–529.

Weber, J., Lyseng-Williamson, K.A., Scott, L.J., 2008. Aripiprazole: in major depressive disorder. CNS Drugs 22, 807–813.

Yao, J.K., Reddy, R.D., van Kammen, D.P., 2001. Oxidative damage and schizophrenia: an overview of the evidence and its therapeutic implications. CNS Drugs 15, 287–310.

Yoo, A.S., McLarnon, J.G., Xu, R.L., Lee, Y.B., Krieger, C., Kim, S.U., 1996. Effects of phorbol ester on intracellular $Ca^{2+}$ and membrane currents in cultured human microglia. Neurosci. Lett. 218, 37–40.

Zhang, X.Y., Chen da, C., Xiu, M.H., Wang, F., Qi, L.Y., Sun, H.Q., Chen, S., He, S.C., Wu, G.Y., Haile, C.N., Kosten, T.A., Lu, L., Kosten, T.R., 2009a. The novel oxidative stress marker thioredoxin is increased in first-episode schizophrenic patients. Schizophr. Res. 113, 151–157.

Zhang, X.Y., Zhou, D.F., Qi, L.Y., Chen, S., Cao, L.Y., Chen da, C., Xiu, M.H., Wang, F., Wu, G. Y., Lu, L., Kosten, T.A., Kosten, T.R., 2009b. Superoxide dismutase and cytokines in chronic patients with schizophrenia: association with psychopathology and response to antipsychotics. Psychopharmacology (Berl) 204, 177–184.

Neuroscience Research 69 (2011) 67–72

Contents lists available at ScienceDirect

Neuroscience Research

journal homepage: www.elsevier.com/locate/neures

# fMRI of patients with social anxiety disorder during a social situation task

Tomohiro Nakao[a,*], Hirokuni Sanematsu[a], Takashi Yoshiura[b], Osamu Togao[b], Keitaro Murayama[a], Mayumi Tomita[c], Yusuke Masuda[c], Shigenobu Kanba[a]

[a] Department of Neuropsychiatry, Graduate School of Medical Sciences, Kyushu University, 3-1-1 Maidashi, Higashi-ku, Fukuoka 812-8582, Japan
[b] Department of Clinical Radiology, Graduate School of Medical Sciences, Kyushu University, 3-1-1 Maidashi, Higashi-ku, Fukuoka 812-8582, Japan
[c] Clinical Psychology and Community Studies, Graduate School of Human-Environment Studies, Kyushu University, 3-1-1 Maidashi, Higashi-ku, Fukuoka 812-8582, Japan

ARTICLE INFO

*Article history:*
Received 13 August 2010
Received in revised form
23 September 2010
Accepted 24 September 2010
Available online 1 October 2010

*Keywords:*
Social anxiety disorder (SAD)
functional MRI
Social situation
Posterior cingulate cortex
Cerebellum
Cognition
Emotion

ABSTRACT

Previous functional neuroimaging studies found that the amygdala and other limbic regions may play a substantial role in social anxiety disorder (SAD). However, more widely distributed large-scale brain systems may be involved in cognitive processing in SAD patients when confronted with social situations. We employed functional MRI (fMRI) to investigate local brain activation of patients with SAD ($n=6$) and healthy controls (HC, $n=9$) during cognitive work. During fMRI scanning, subjects performed a social situation task using a block design paradigm in which the task and control trials were performed by turn. The patients with SAD showed higher anxiety levels during scanning in all social situations. The HC group showed greater common activation in the posterior cingulate cortex (PCC), cuneus, occipital gyrus, and cerebellum. Although the patients with SAD showed activation patterns similar to that of the HC group, they showed comparatively significant decreased activation in the left cerebellum, left precuneus, and bilateral PCC. The present study demonstrates that SAD may involve dysfunction of a broad neuronal network including the limbic system, parieto-posterior cortex and cerebellum. The findings contribute to previous findings that revealed abnormal activities of emotion-related regions including the amygdala and insular cortex during facial perception in SAD.



## 1. Introduction

Social anxiety disorder (SAD), which is classified as a phobic disorder in the Diagnostic and Statistical Manual of Mental Disorder IV (DSM-IV) (American Psychiatric Association, 1994), is one of the anxiety disorders characterized by fear of public scrutiny and social interactions. Recently, SAD has been become known as a common disease and is garnering increased attention as an impairing condition. The National Comorbidity Survey-Replication estimates the lifetime prevalence of DSM-IV SAD as 12.1%, respectively (Kessler et al., 2005). Patients with SAD show emotional and physical symptoms such as fear, racing heart, sweating, and trembling. They are withdrawn when performing tasks such as speaking, eating, and writing in public and expressing opinions in unfamiliar social settings. Moreover, their social fears and avoidance extend far beyond the relatively common sphere of concern.

Although family and genetic studies (Stein et al., 1998, 2001) have contributed to elucidation of the pathology of SAD, its pathophysiologic mechanisms remain obscure. Recently, a neurobiological basis for SAD has attracted considerable attention. Functional neuroimaging techniques, especially PET, SPECT, and fMRI, have revealed biological backgrounds of SAD (Amir et al., 2005; Furmark et al., 2002; Phan et al., 2006; Stein et al., 2002; Tillfors et al., 2001). These functional neuroimaging studies revealed that the amygdala and other regions including the insular cortex and hippocampus may play a substantial role in SAD. Increased fear and anxiety may be associated with increased regional cerebral blood flow (rCBF) in these areas, which is consistent with most studies identifying the amygdala, insular cortex, and hippocampus as important in emotional processing. However, there are also consistent foci of activation abnormalities in the lateral frontal, anterior cingulate, middle occipital, and parietal cortices and cerebellum, suggesting that more widely distributed large-scale brain systems may be involved in anxiety disorders such as OCD (Menzies et al., 2008). This could be because the brain abnormalities responsible for anxiety disorders are present at a brain network level, with abnormalities across several different regions accounting for impairments in cognitive processing. Thus, cognitive processing may also be important in understanding the pathophysiology of SAD.

There are, however, few studies that employed cognitive tasks other than perception of facial expressions as a stimulant task. In the present study, we hypothesized that the pathological anxiety of SAD might be related not only to perception of facial expressions

* Corresponding author. Tel.: +81 92 642 5623; fax: +81 92 642 5644.
*E-mail address:* tomona@npsych.med.kyushu-u.ac.jp (T. Nakao).

0168-0102/$ – see front matter © 2010 Elsevier Ireland Ltd and the Japan Neuroscience Society. All rights reserved.
doi:10.1016/j.neures.2010.09.008

but also to the social situations that patients are confronted with. To clarify brain areas that are involved in anxiety in social situations, we administered a social situation task during functional magnetic resonance imaging (fMRI) to healthy controls and patients with SAD.

## 2. Methods

### 2.1. Subjects

The subjects comprised six patients with SAD and nine healthy controls. The two groups did not differ with respect to sex ratio, age, and handedness. The SAD patients were recruited from outpatients of the Department of Neuropsychiatry, Kyushu University Hospital. We included SAD patients who had no comorbid mental disorders. The patients included were 18–60 years old and had a primary SAD diagnosis that was confirmed to meet DSM-IV criteria by using SAD and the psychosis subsections of the Structured Clinical Interview for DSM-IV-Patient edition (SCID-P, Japanese language edition) (First et al., 1996). All patients showed significant symptoms despite previous and current treatments. Patients who displayed a comorbid axis I diagnosis, neurological disorder, head injury, serious medical condition, or history of drug/alcohol addiction were excluded.

Depressive symptoms were assessed using the 17-item Hamilton Depression Rating Scale (HDRS) (Hamilton, 1960), and patients who showed a total HDRS score of more than 18 points were excluded. Spielberger, C.D Intelligence was assessed by using the Wechsler Adult Intelligence Scale-Revised (WAIS-R) (Wechsler, 1981), and patients with a total IQ of less than 80 were excluded. Each patient also completed the 40-item State-Trait Anxiety Inventory (STAI) (Spielberger et al., 1970) and Liebowitz Social Anxiety Scale, SAD severity (LSAS, 24 items, 144 pts full score) (Liebowitz, 1987) to assess the severity of general and social anxiety symptoms. The handedness of each patient was determined using the Edinburgh handedness inventory (Oldfield, 1971). Concerning treatment history, four patients are treatment-naïve and had not taken any psychotropic medication before they entered this study. The remaining two patients were taking antidepressant drugs at least one year before entering the study. One patient received milnacipran, and the other received amoxapine.

Exclusion criteria for the healthy controls (HC) were any axis I diagnosis, neurological illness, other disorders of the central nervous system, and a history of substance abuse. Participants with LSAS scores higher than 20 points were excluded. Depressive symptoms were assessed using HDRS, and the total HDRS score of each control subject was less than 18 (in the normal to mildly depressed range).

### 2.2. Procedure for fMRI

Functional magnetic resonance imaging (fMRI) was used to investigate local brain activation during cognitive work. Each participant was scanned using a 1.5-T MRI scanner (Magnetom Symphony Siemens, Erlangen, Germany) and standard head coil. A high-resolution T1-weighted scan was then acquired for anatomical reference. Functional images were obtained using a gradient echo-planar sequence (repetition time, 4000 ms; echo time, 50 ms; flip angle, 90°; field-of-view, 230 mm; matrix, 64 × 64; slice thickness, 3 mm; gap, 1 mm; 32 axial slices). Foam padding was used to minimize the motion of the subject's head during imaging.

### 2.3. Social situation task

During fMRI scanning, subjects performed a social situation task. In the task, a series of eight photographs of social situations such as going to a reception, restaurant, or conference were displayed on a video screen at the subject's foot (Table 1). Each photograph was presented 5 s and the participants were required to imagine themselves in the situation. In the task trial, there were 1–7 persons in each scene. In the control trial, the same situations were presented without people. We employed a block design paradigm in which control and task trials were performed by turns. This paradigm comprised ten 40-s periods, which means that task and control conditions repeated five times each (total, 400 s). Each block includes eight scenes that are shown in Table 1. The scenes appeared 5 s each in order as Table 1. All of the eight experimental stimuli are compared with all of the control stimuli. Parameters of image acquisition were chosen to optimize the BOLD contrast. The anxiety levels (0–3) of both task condition and control condition for each scene were assessed before scanning.

**Table 2**
Clinical characteristics of patients with SAD and healthy controls.

| | SAD ($n = 6$) | Healthy control ($n = 9$) |
|---|---|---|
| Age | 31.7 ± 7.9 | 32.8 ± 5.0 |
| Sex (m/f)[a] | 4/2 | 6/3 |
| Phobia/anxiety | 42.2 ± 12.8 | 8.0 ± 4.2*** |
| Avoidance | 38.7 ± 12.1 | 4.3 ± 3.8*** |
| Total | 80.8 ± 24.1 | 12.3 ± 6.9*** |
| Trait anxiety | 62.2 ± 12.2 | 34.4 ± 10.4** |
| State anxiety | 53.2 ± 13.3 | 34.3 ± 8.5* |
| 17 items | 8.3 ± 6.4 | 0.3 ± 0.7** |
| Total | 12.7 ± 9.4 | 0.7 ± 1.0* |
| Control[b] | 5.2 ± 3.5*** | 0.7 ± 1.0** |
| Task[b] | 13.2 ± 5.7*** | 1.7 ± 1.2*** |

LSAS: Liebowitz Social Anxiety Scale, STAI: State-Trait Anxiety Inventory, HDRS: Hamilton Depression Rating Scale.
Mann–Whitney $U$, ***$p < 0.001$ **$p < .01$ *$p < .05$.
[a] Fisher's exact test.
[b] ANOVA test, ***$p < 0.001$ **$p < 0.01$.

### 2.4. Statistical analysis

Clinical characteristics of the patients group and the HC group were compared using Mann–Whitney $U$ test and Fisher's exact test. Concerning the social situation task, we employed analysis of variance (ANOVA) test to examine statistical difference of total anxiety levels between the task and control condition for both the SAD and HC group. We also employed ANOVA test to examine statistical difference of evoked anxiety levels for both the task and control of the eight social scenes.

For analysis of imaging results, Statistical Parametric Mapping (SPM) 2 (Wellcome Department of Cognitive Neurology, London, UK) software was used. To correct for motion of the subject's head, functional images from each individual were realigned to the first image in the series using 6-parameter spatial transformation. After realignment, functional images were spatially normalized with the Montreal Neurological Institute EPI template, and then convolved in space with a three-dimensional isotropic Gaussian kernel (full width at half maximum = 12 mm) for smoothing. The effect of the symptom provocation task was estimated at each and every voxel using a general linear model. Voxel values for the task versus control contrast yielded a statistical parametric map of the $t$ statistic, and the values were then normalized to $Z$ scores. A corresponding contrast image for each patient was also created for the group analysis.

Common activation maps of each SAD and HC group were created using random-effects model of SPM after generating individual images. After generating images of all subjects, we used a one-sample $t$ test to compare task versus control conditions. Voxel-wise significance thresholds of $p < 0.001$ (uncorrected) were used. Only clusters with more than 10 voxels were included.

For comparison of activation maps between the SAD and HC groups, task-versus-control contrast images of all participants were obtained for each group, and the contrast images of each group were compared using random-effects model. Voxel-wise, significance thresholds of $p < 0.001$ (uncorrected) were used. Only clusters with more than 10 voxels were included.

## 3. Results

Clinical characteristics of the two groups are shown in Table 2. Patients with SAD showed significantly higher scores than HCs on the LSAS (SAD, 80.8 ± 24.1; HC, 12.3 ± 6.9, $p < 0.001$, Mann–Whitney $U$). Patients with SAD showed mild depressive

**Table 1**
Social situation task.

| | Place | Member | Situation |
|---|---|---|---|
| Scene 1 | Conference room | Seven company employees | You are requested to express your opinion in the meeting. |
| Scene 2 | Public office | A female receptionist | You have to ask her about documents. |
| Scene 3 | Reception room | A person in a high position | You have to tell him important business matter. |
| Scene 4 | Conference room | Four company employees | You are requested to express your opinion at the meeting. |
| Scene 5 | Reception desk | Three female receptionists | You have to sign your name at the desk. |
| Scene 6 | Meeting room | Three persons | You have to read a textbook. |
| Scene 7 | Meeting room | Three persons | You are requested to express your opinion at the meeting. |
| Scene 8 | Restaurant | A chef | You eat a meal in the presence of others. |